Electronic Supplementary Material (ESI) for Polymer Chemistry.

Supporting Information:

Pro-organic radical contrast agents ("pro-ORCAs") for real-time MRI of pro-drug activation in biological systems

Hung V.-T. Nguyen,[1,5,6,7,10] Alexandre Detappe,[5,6,7,8,10] Peter Harvey,[2] Nolan Gallagher,[1] Clelia Mathieu,[6,7] Michael P. Agius,[6,7] Oksana Zavidij,[6,7] Wencong Wang,[1] Yivan Jiang,[1] Andrzej Rajca,[9] Alan Jasanoff,[2,3,4] Irene M. Ghobrial,[6,7] P. Peter Ghoroghchian,[5,6,7,*] and Jeremiah A. Johnson[1,5,*]

[1]*Department of Chemistry,* [2]*Department of Biological Engineering,* [3]*Department of Brain and Cognitive Sciences,* [4]*Department of Nuclear Science and Engineering, and* [5]*David H. Koch Institute for Integrative Cancer Research, Massachusetts Institute of Technology, 77 Massachusetts Avenue, Cambridge, Massachusetts 02139, United States*

[6]*Department of Medical Oncology, Dana-Farber Cancer Institute, 450 Brookline Avenue, Boston, Massachusetts 02215, United States*

[7]*Harvard Medical School, 25 Shattuck Street, Boston, Massachusetts 02115, United States*

[8]*Centre Paul Strauss, 3 Rue de la Porte de l'Hopital, 67000 Strasbourg, France*

[9]*Department of Chemistry, University of Nebraska, Lincoln, Nebraska 68588, United States*

[10]*These authors contributed equally to this work*

[*]*Correspondence: jaj2109@mit.edu (J.A.J.) and ppg@mit.edu (P.P.G.)*

Table of Contents

Section A. Figures Cited in the Main Text

Spectra Data for chex-PC-MM

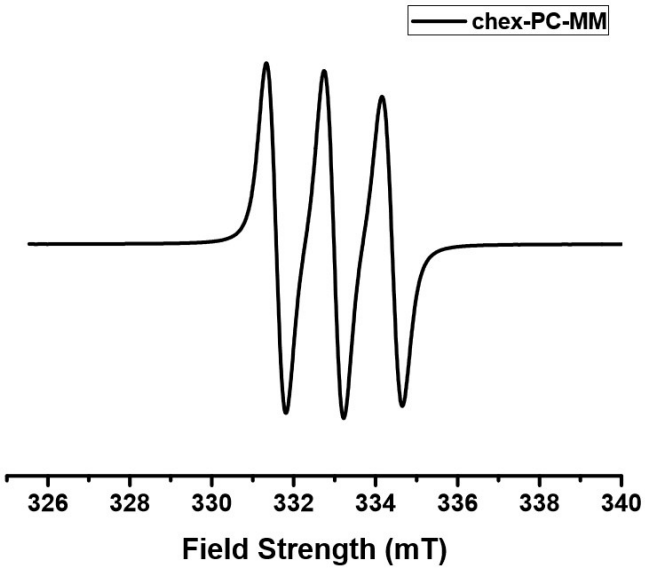

Figure S1. EPR spectrum of **chex-PC-MM**.

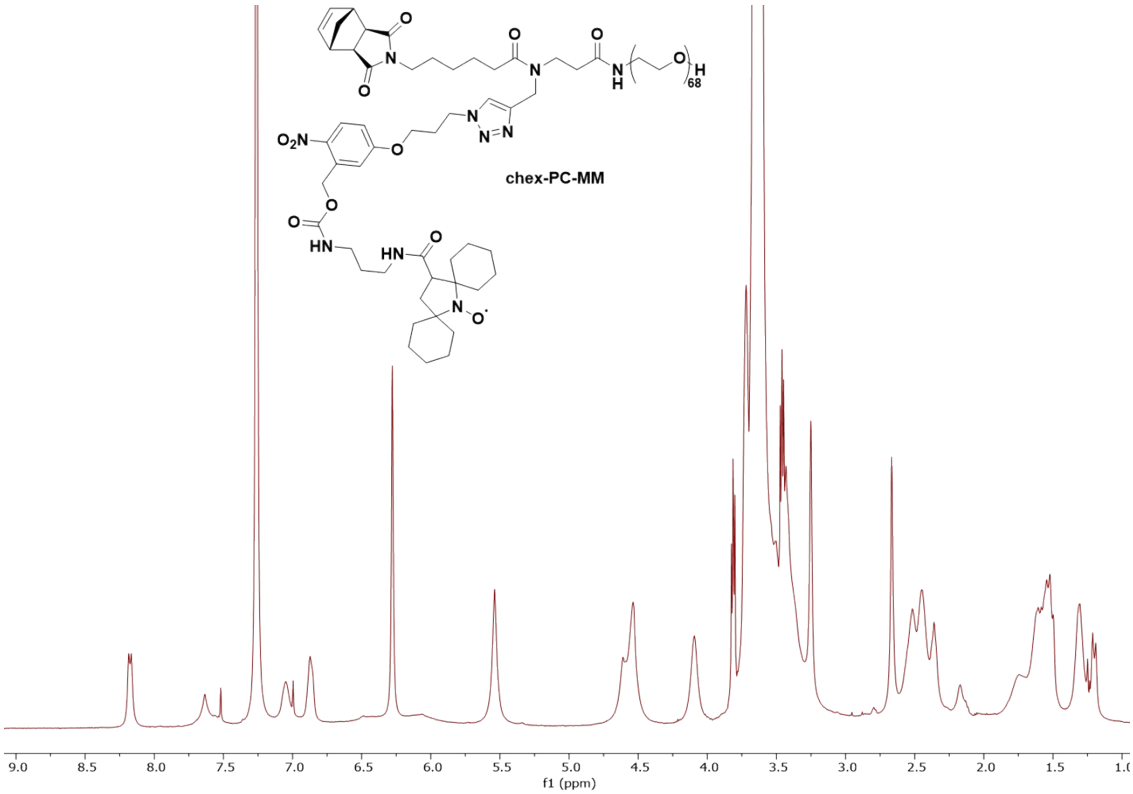

Figure S2. ^{1}H NMR spectrum of **chex-PC-MM** in $CDCl_3$.

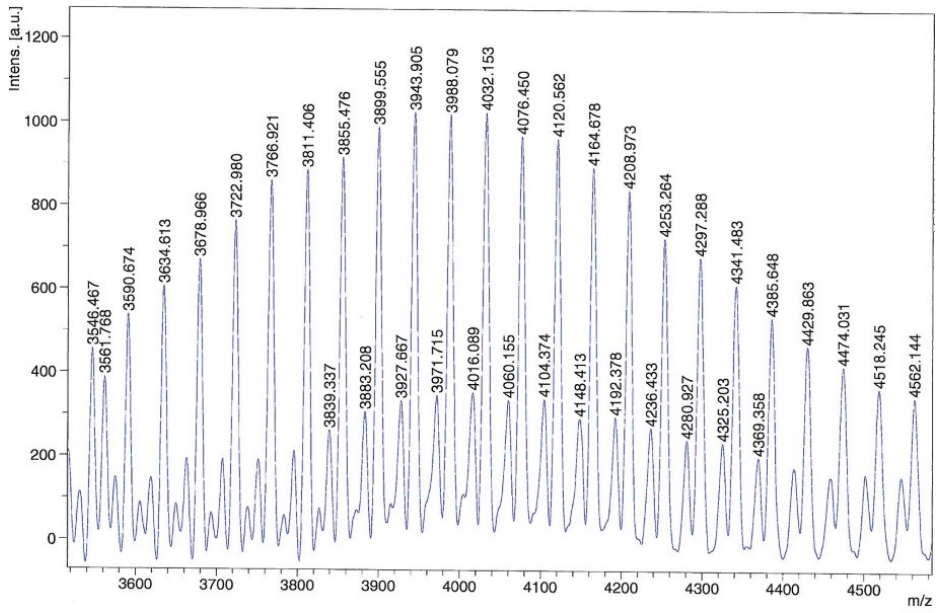

Figure S3. MALDI-TOF spectrum of **chex-PC-MM**. $C_{182}H_{333}O_{77}N_{10}Li$: calcd m/z = 3898.51; Found: 3899.555 $[M + Li]^+$. $C_{182}H_{333}O_{77}N_{10}K$: calcd m/z = 3930.45; Found: 3927.667 $[M + K]^+$.

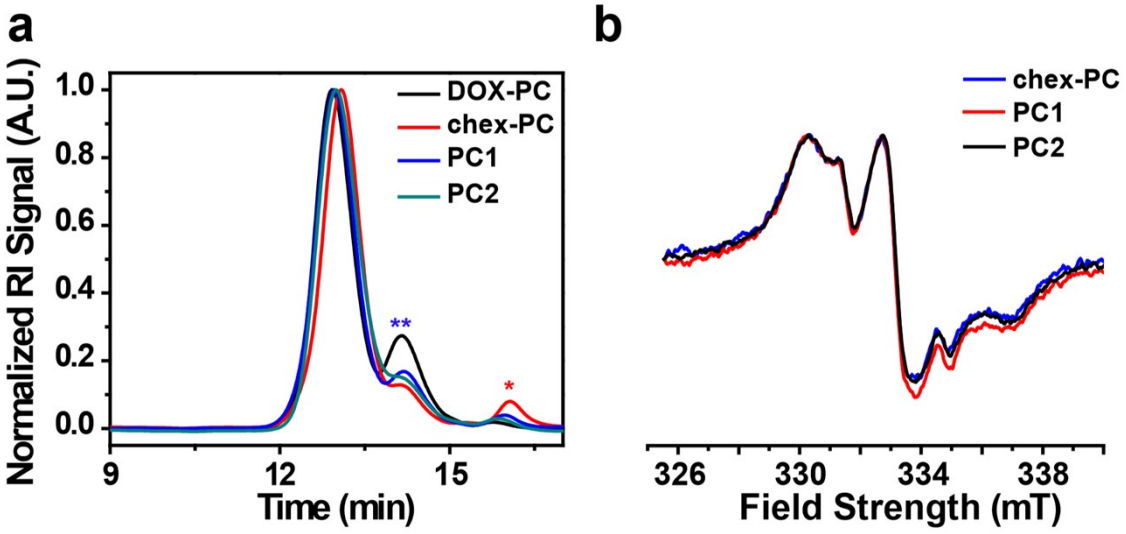

Figure S4. (a) GPC Traces of **DOX-PC**, **chex-PC**, **PC1**, and **PC2**. *indicates residual MM; **denotes uncoupled bottlebrush. In all cases, reaction conversions were ≥ 90% by mass. (b) EPR Spectra of **chex-PC**, **PC1**, and **PC2**. For all BASP EPR spectra, spin concentrations of ≥ 85% were determined.

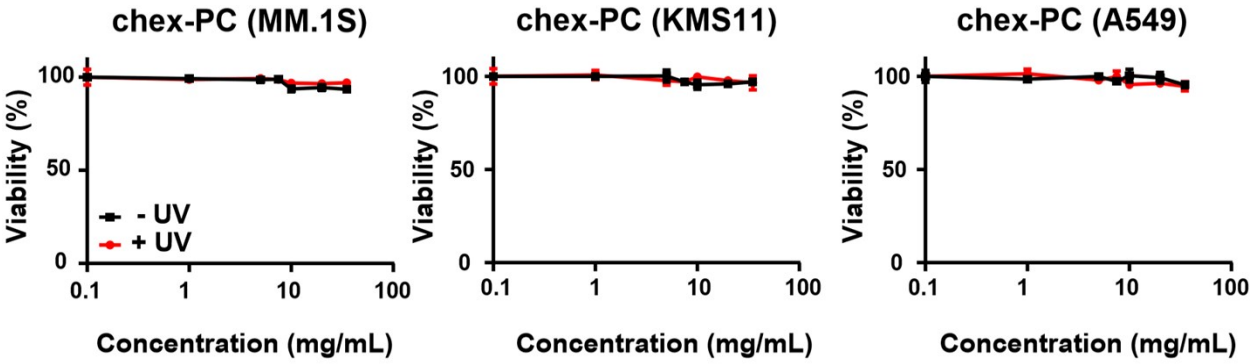

Figure S5. *In vitro* cytotoxicity evaluation of **chex-PC**. Cell viability assay for lung adenocarcinoma (A549) and multiple myeloma (MM.1S and KMS11) cells. Cell lines were incubated with varying concentrations of **chex-PC** for 48h and characterized by CellTiter-Glo (n = 3 technical replicates per data point). No toxicity was observed until high BASP concentrations. Data are represented as mean ± SEM.

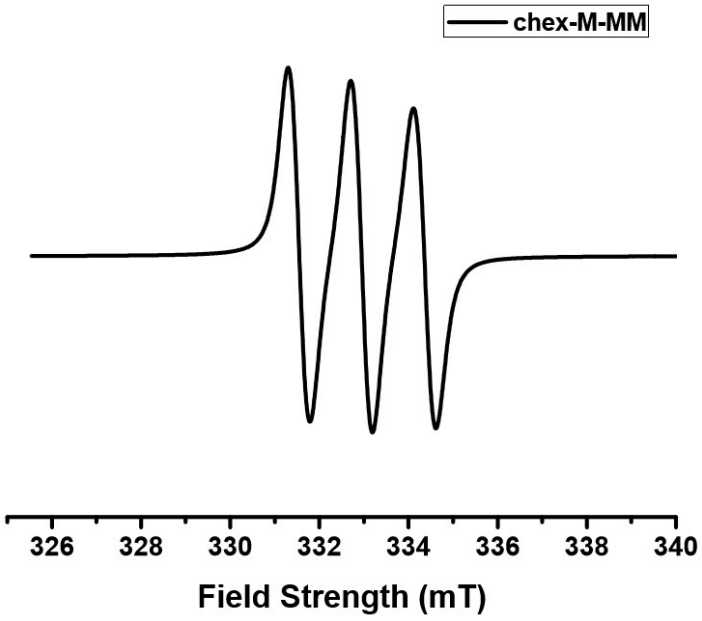

Figure S6. EPR Spectrum of **chex-M-MM**.

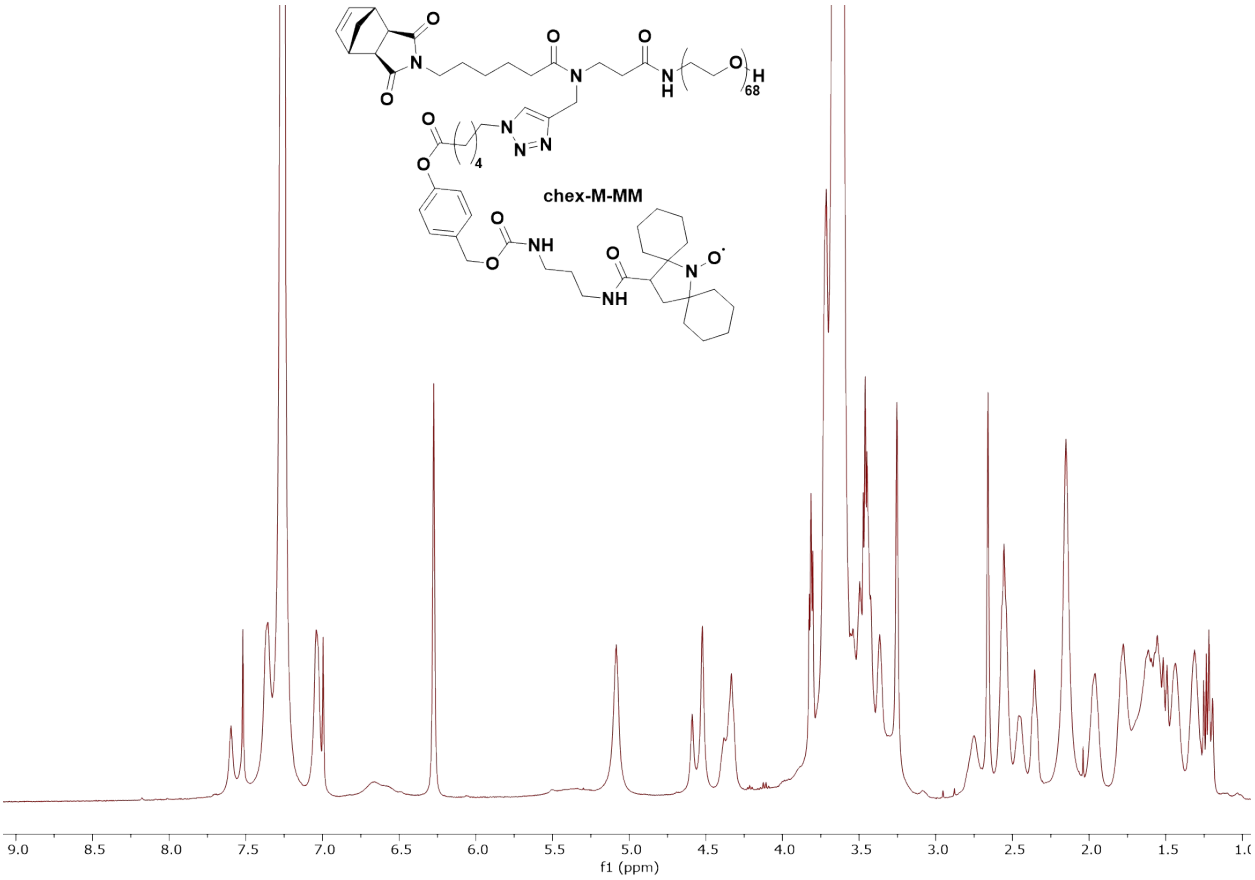

Figure S7. ^{1}H NMR Spectrum of **chex-M-MM** in $CDCl_3$.

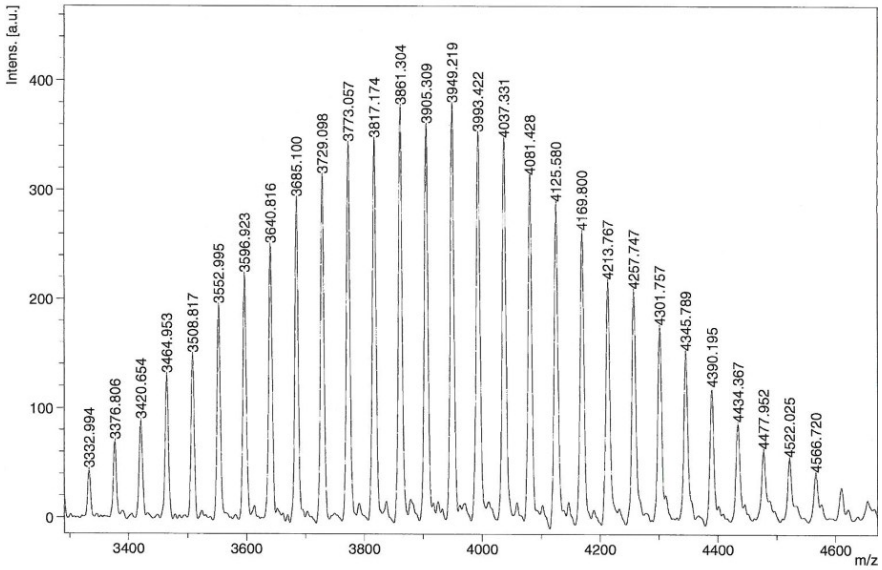

Figure S8. MALDI-TOF Spectrum of **chex-M-MM**. $C_{179}H_{327}O_{73}N_9$: calcd m/z = 3771.46; Found: 3773.057 $[M + H]^+$.

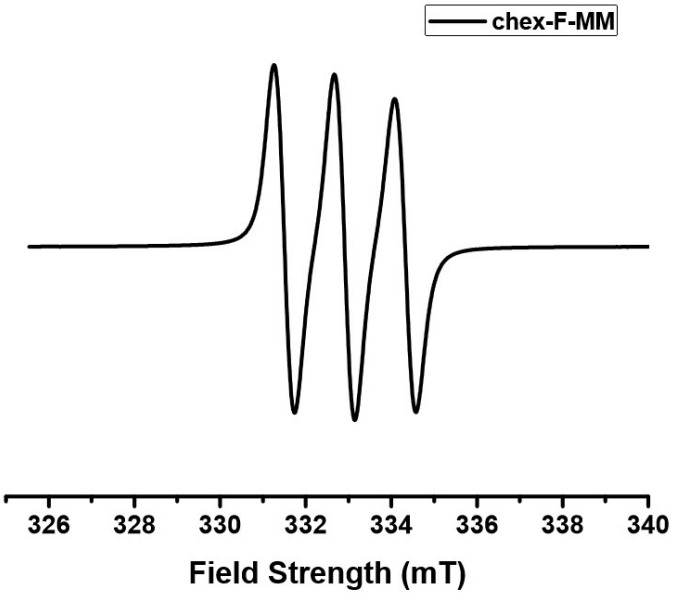

Figure S9. EPR Spectrum of **chex-F-MM**.

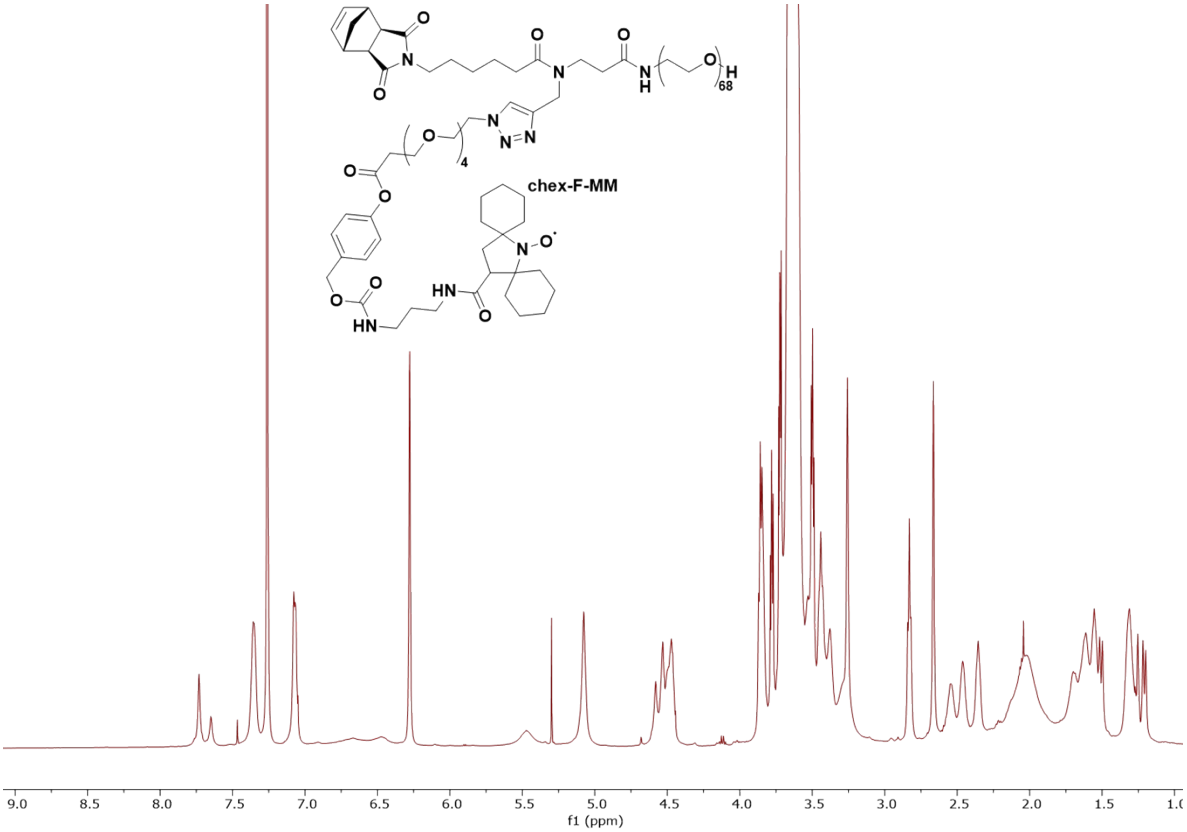

Figure S10. ^{1}H NMR Spectrum of **chex-F-MM** in $CDCl_3$.

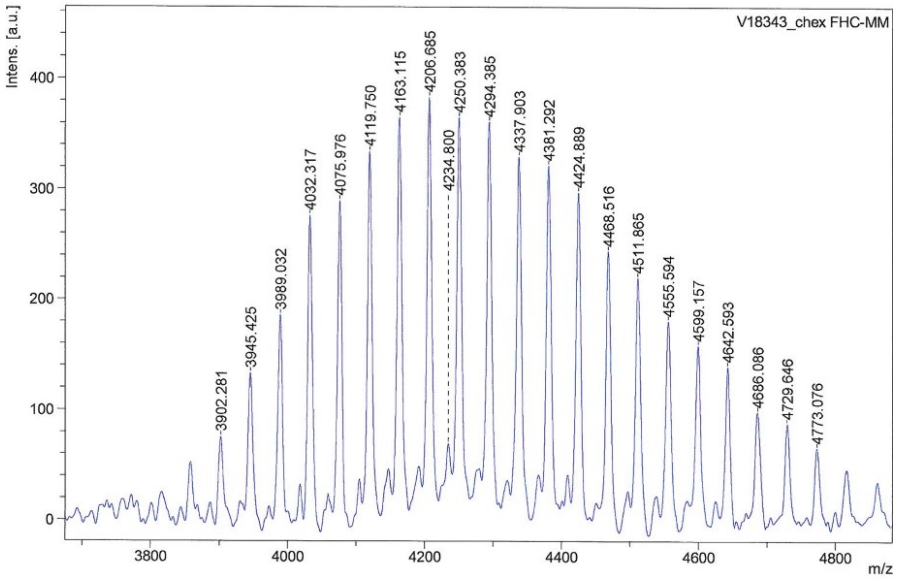

Figure S11. MALDI-TOF Spectrum of **chex-F-MM**. $C_{194}H_{356}O_{82}N_9K$: calcd m/z = 4163.61; Found: 4163.115 $[M + K]^+$. $C_{198}H_{364}O_{84}N_9Na$: calcd m/z = 4235.70; Found: 4234.800 $[M + Na]^+$.

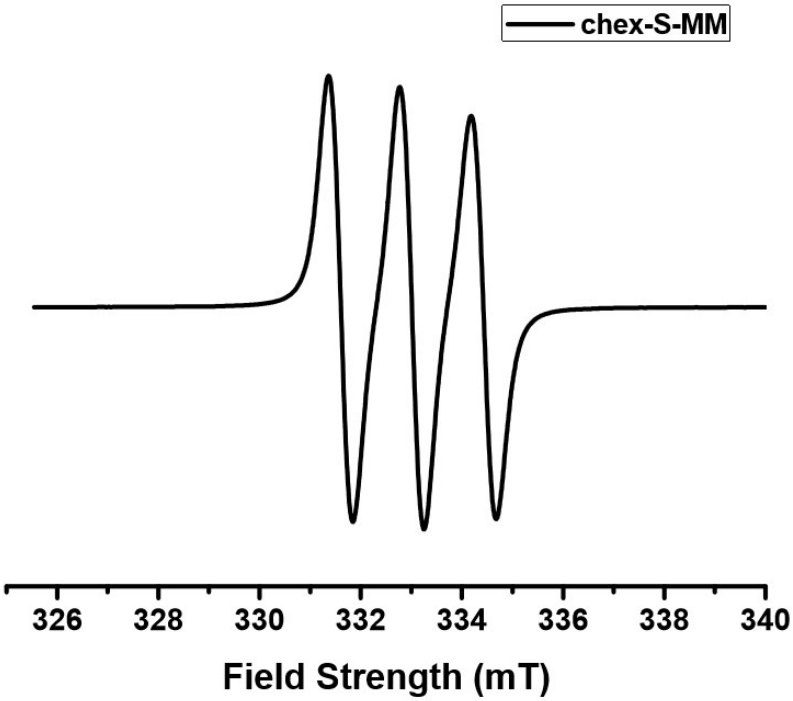

Figure S12. EPR Spectrum of **chex-S-MM**.

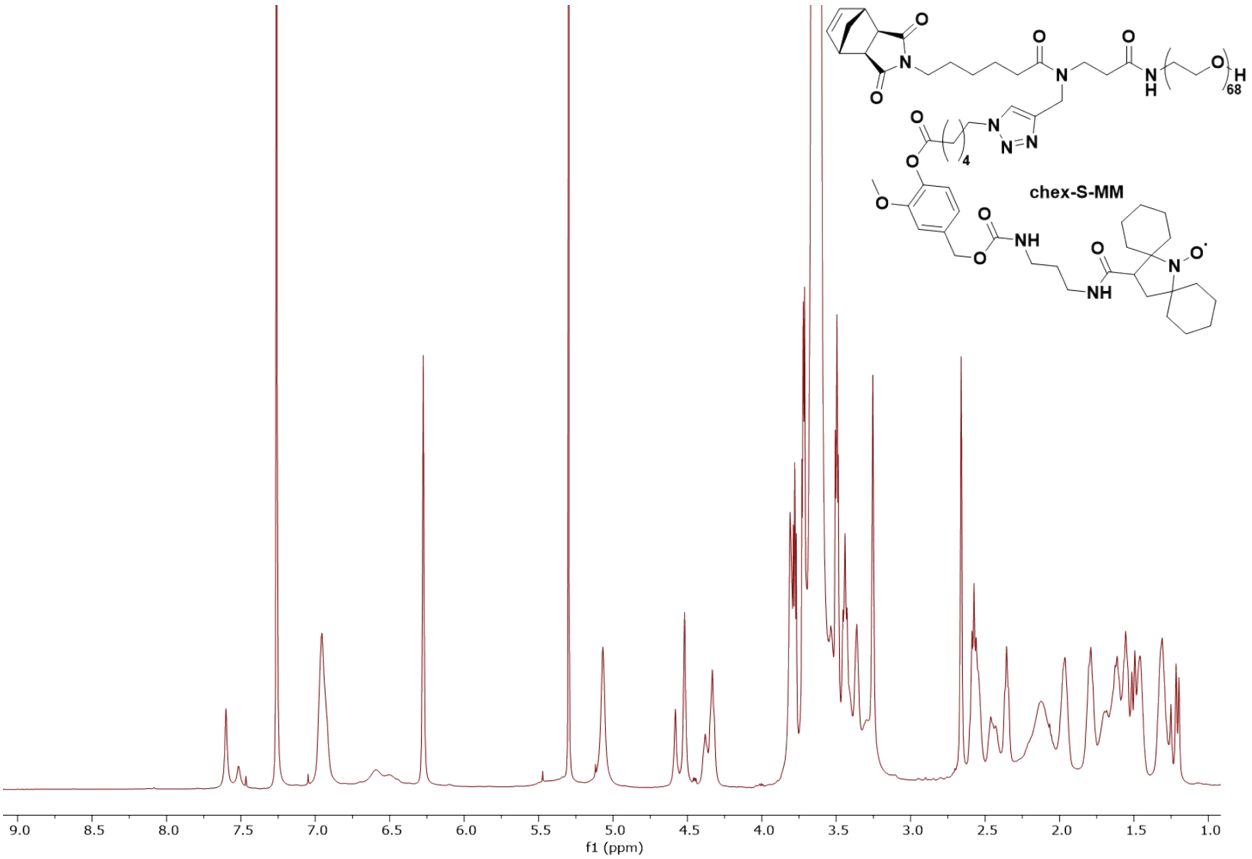

Figure S13. ^{1}H NMR Spectrum of **chex-S-MM** in $CDCl_3$

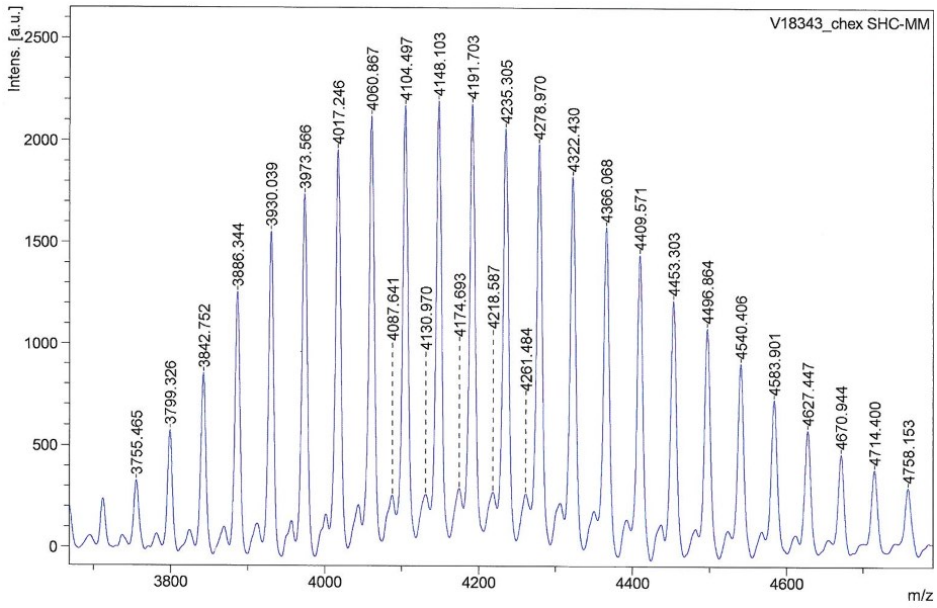

Figure S14. MALDI-TOF Spectrum of **chex-S-MM**. $C_{196}H_{360}O_{82}N_9K$: calcd m/z = 4191.66; Found: 4191.703 $[M + K]^+$. $C_{191}H_{351}O_{80}N_9Na$: calcd m/z = 4175.69; Found: 4174.693 $[M + Na]^+$.

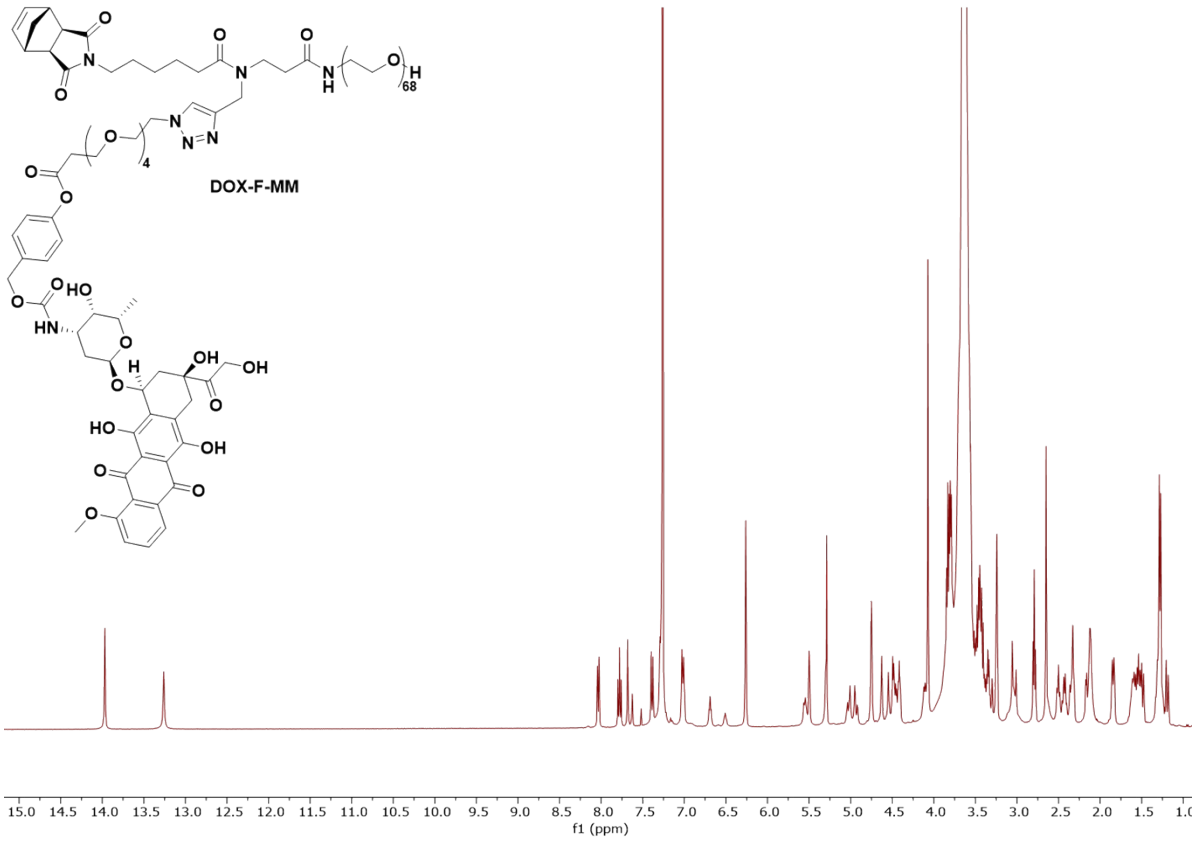

Figure S15. ^{1}H NMR Spectrum of **DOX-F-MM** in $CDCl_3$.

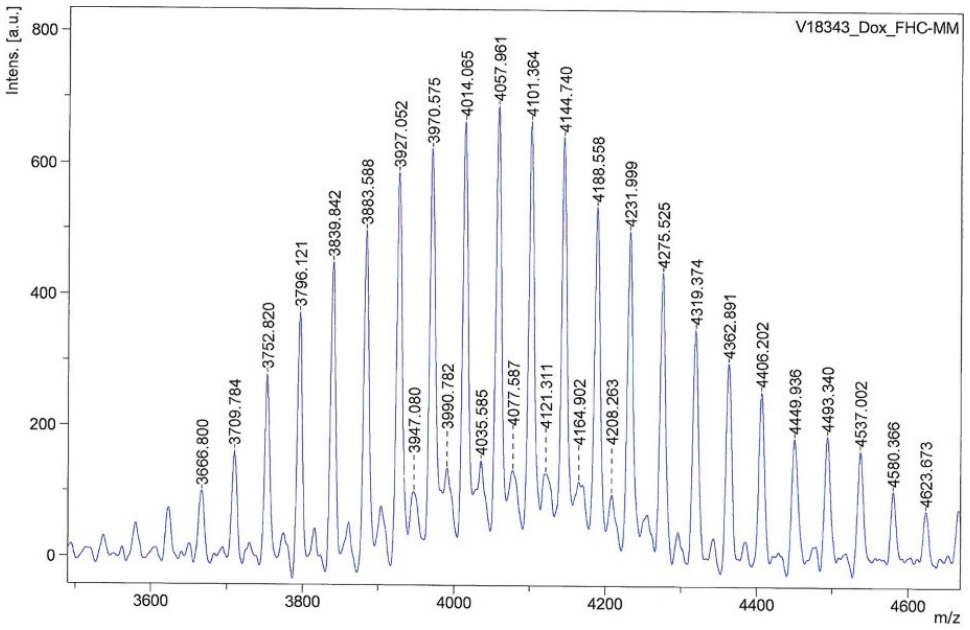

Figure S16. MALDI-TOF Spectrum of **DOX-F-MM**. $C_{195}H_{340}O_{88}N_7$: calcd m/z = 4188.48; Found: 4188.558 $[M + H_3O]^+$. $C_{195}H_{340}O_{88}N_7K$: calcd m/z = 4208.42; Found: 4208.263 $[M + K]^+$.

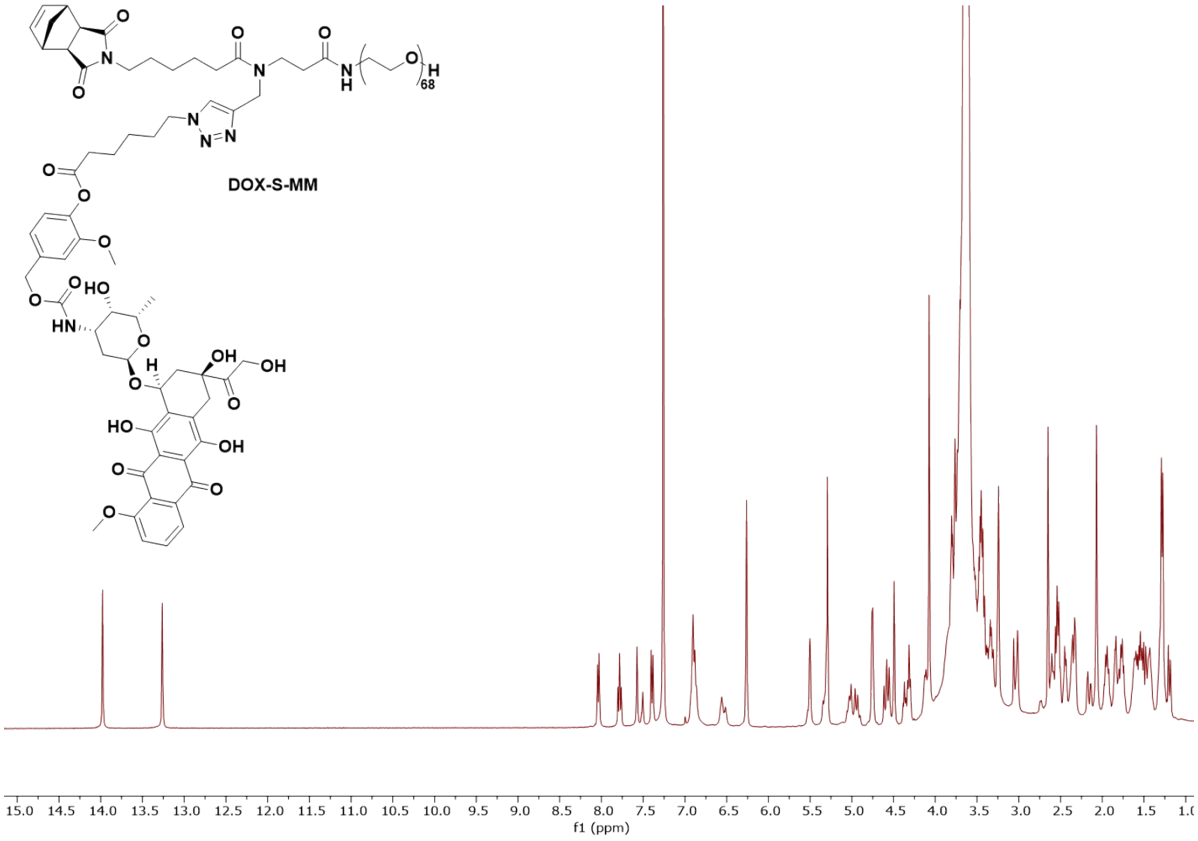

Figure S17. ^{1}H NMR Spectrum of **DOX-S-MM** in $CDCl_3$.

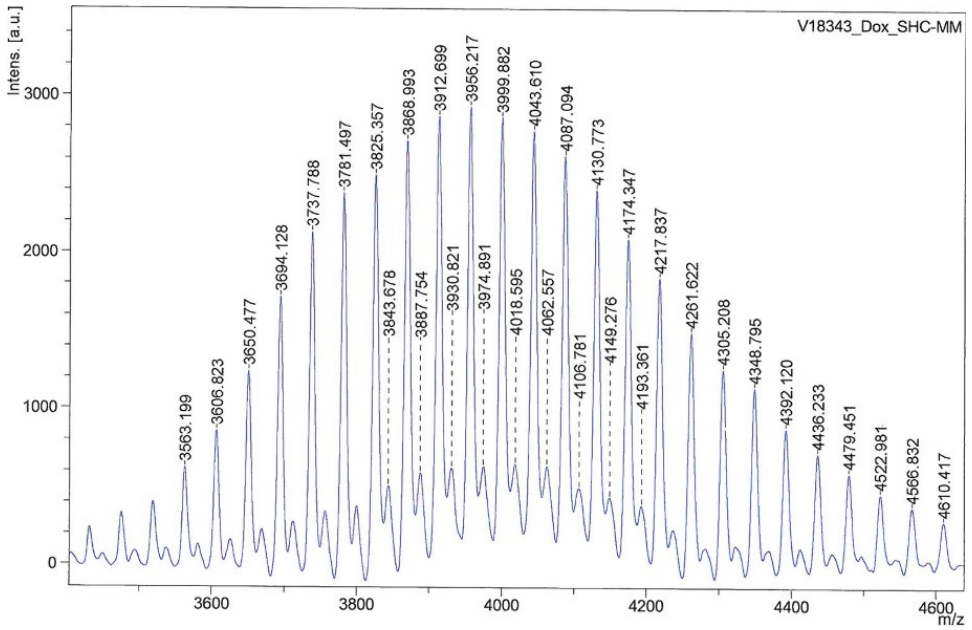

Figure S18. MALDI-TOF Spectrum of **DOX-S-MM**. $C_{185}H_{317}O_{81}N_7Na$: calcd m/z = 3956.31; Found: 3956.217 $[M + Na]^+$. $C_{189}H_{325}O_{83}N_7K$: calcd m/z = 4060.34; Found: 4062.781 $[M + K]^+$.

Table S1. Characterization of the release kinetics in PBS for HC-MMs.

MM Payload	Relative Rate	$k \times 10^3$ (h^{-1})	$t_{1/2}$ (h)	R^2	$t_{1/2}$ (chex/DOX)
DOX	F	21.26	32.6	0.977	2.58
chex	F	8.23	84.2	0.992	
DOX	M	8.95	77.5	0.996	2.08
chex	M	4.31	160.9	0.975	
DOX	S	3.62	191.4	0.995	2.22
chex	S	1.63	424.2	0.990	

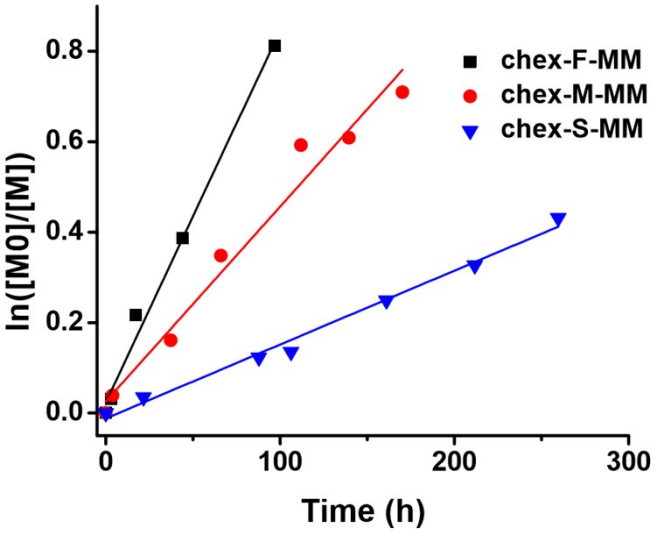

Figure S19. Release kinetics of chex in PBS of **chex-F-MM**, **chex-M-MM**, and **chex-S-MM**, as determined by LC-MS.

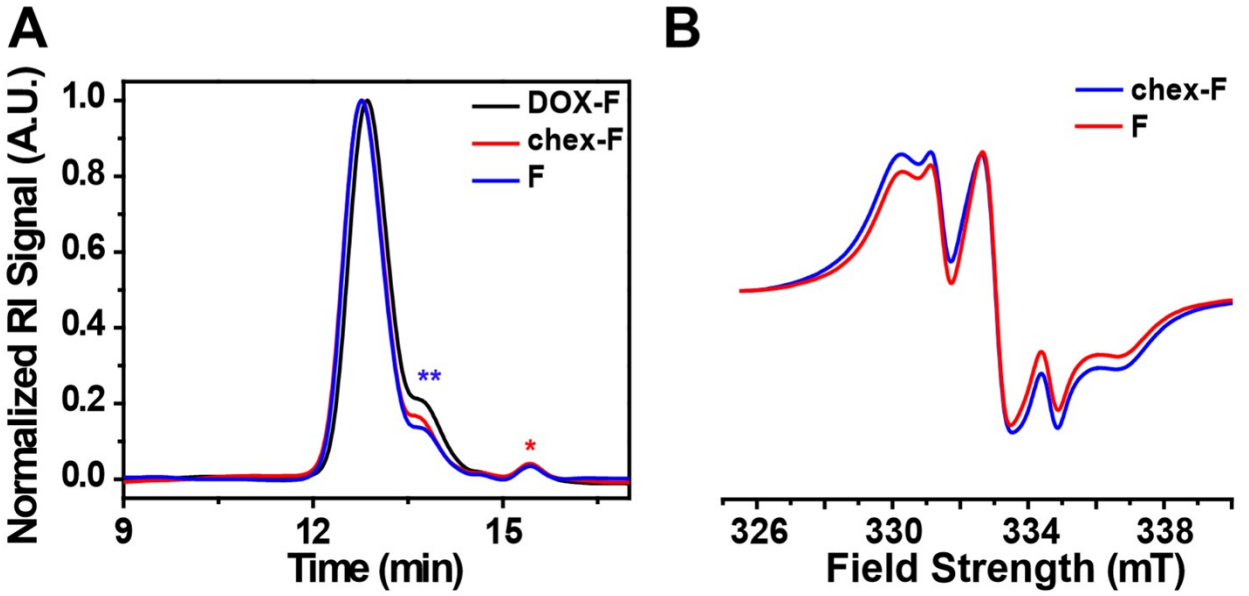

Figure S20. (a) GPC Traces of **DOX-F**, **chex-F**, and **F**. *indicates residual MM; **denotes uncoupled bottlebrush. In all cases, reaction conversions were ≥ 90% by mass. (b) EPR Spectra of **chex-F** and **F**. For all BASP EPR spectra, spin concentrations of ≥ 85% were determined.

Spectra Data for M-BASPs

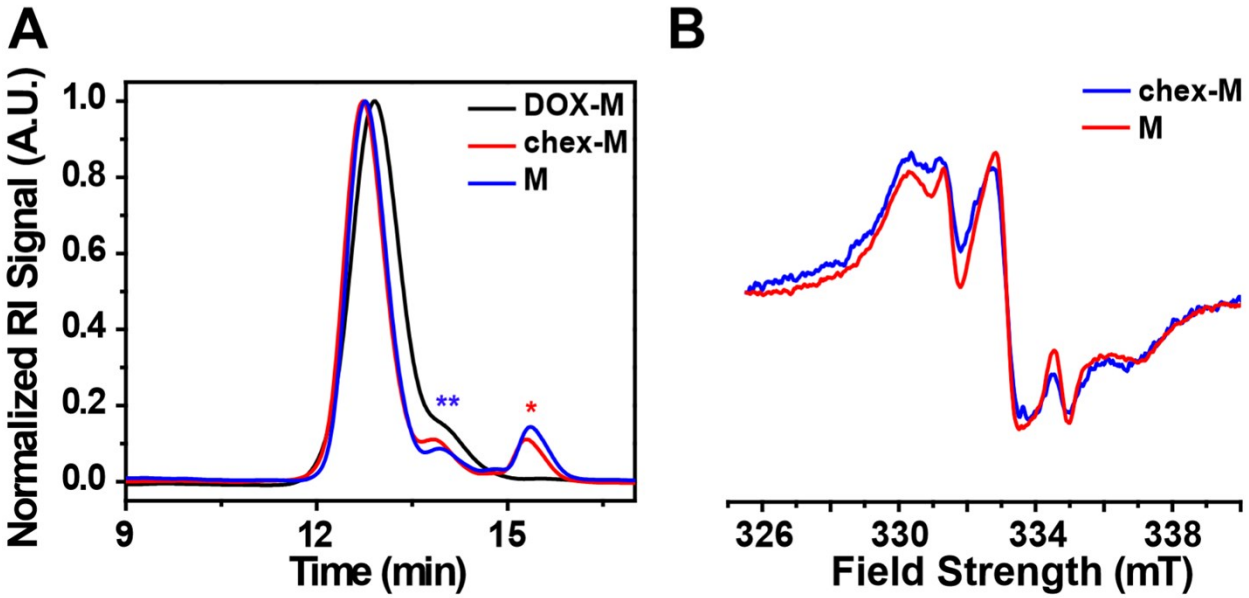

Figure S21. (a) GPC Traces of **DOX-M**, **chex-M**, and **M**. *indicates residual MM; **denotes uncoupled bottlebrush. In all cases, reaction conversions were ≥ 90% by mass. (b) EPR Spectra of **chex-M** and **M**. For all BASP EPR spectra, spin concentrations of ≥ 85% were determined.

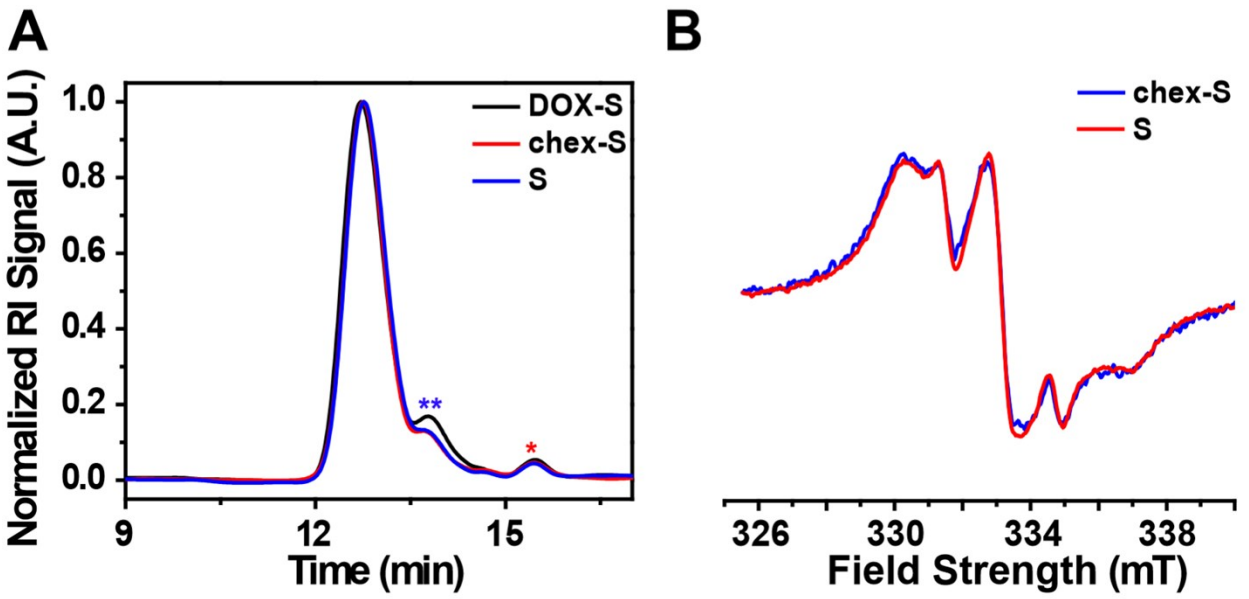

Figure S22. (a) GPC Traces of **DOX-S**, **chex-S**, and **S**. *indicates residual MM; **denotes uncoupled bottlebrush. In all cases, reaction conversions were ≥ 90%. (b) EPR Spectra of **chex-S**, and **S**. For all BASP EPR spectra, spin concentrations of ≥ 85% were determined.

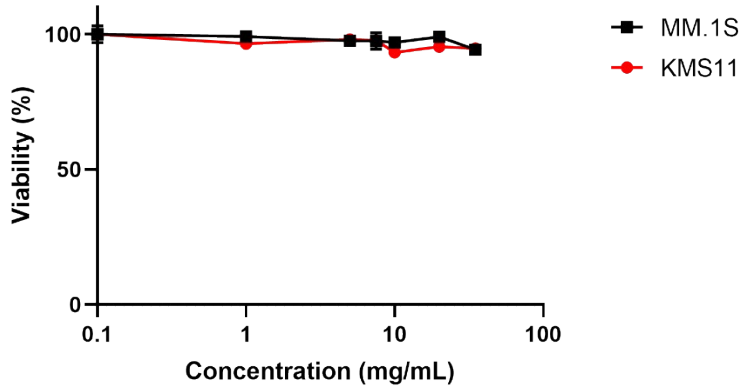

Figure S23. *In vitro* cytotoxicity evaluation of **chex-M**. Cell viability assay for multiple myeloma (MM.1S and KMS11) cells. Cell lines were incubated with varying concentrations of **chex-M** for 48h and characterized by CellTiter-Glo (n = 3 technical replicates per data point). No toxicity was observed until high BASP concentrations. Data are represented as mean ± SEM.

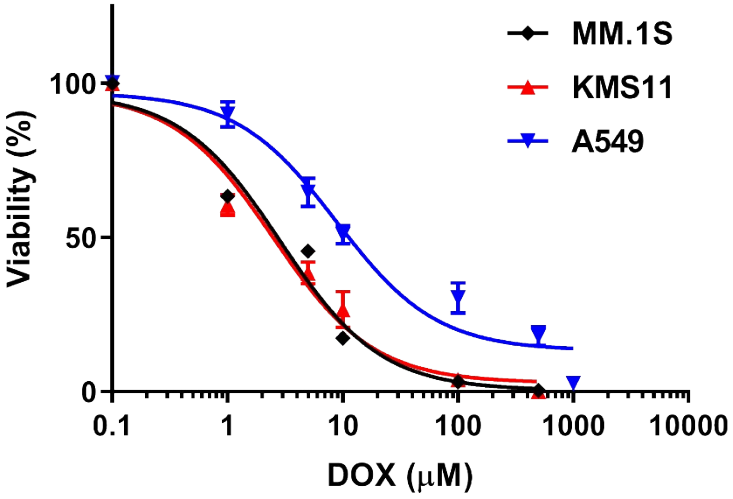

Figure S24. *In vitro* cytotoxicity evaluation of free DOX. Cell viability assay for multiple myeloma (MM.1S and KMS11) and lung adenocarcinoma (A549) cells. Cell lines were incubated with varying concentrations of free DOX for 48h and characterized by CellTiter-Glo (*n* = 3 technical replicates per data point). Data are represented as mean ± SEM.

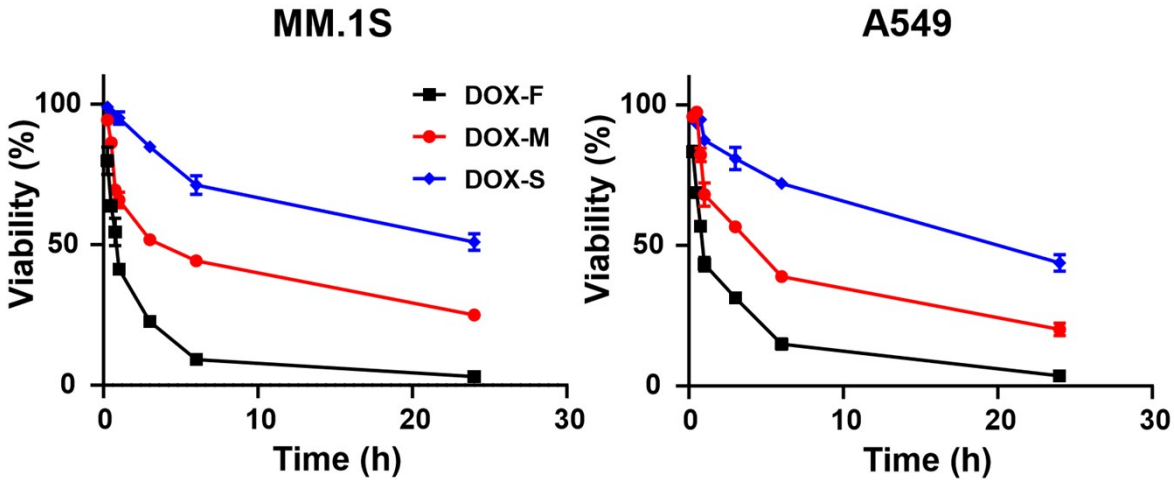

Figure S25. *In vitro* cytotoxicity evaluation of **DOX-F**, **DOX-M**, and **DOX-S** over time at 0.5 mg/mL BASP (83.0 μM, 85.6 μM, and 84.9 μM DOX for **DOX-F**, **DOX-M**, and **DOX-S** respectively). Cell viability assay for lung adenocarcinoma (A549) and multiple myeloma (MM.1S) cells. Cell lines were incubated with 0.5 mg/mL BASPs and characterized by CellTiter-Glo (*n* = 3 technical replicates per data point). Data are represented as mean ± SEM.

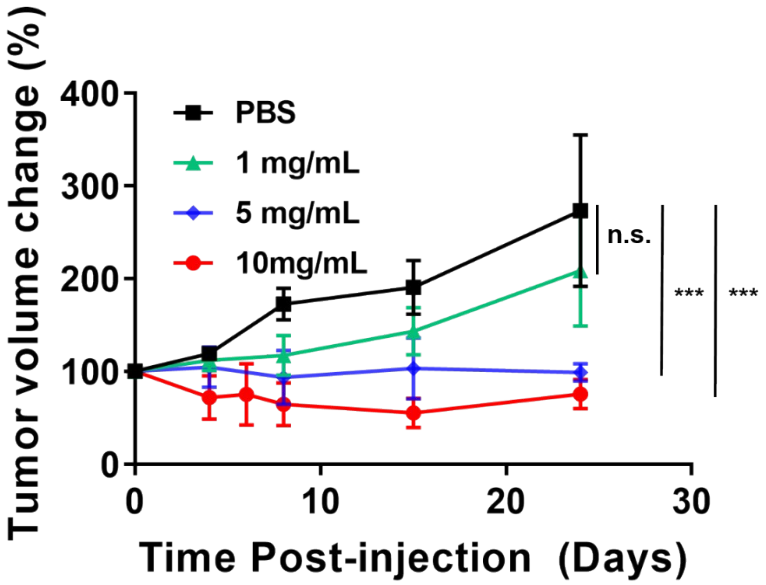

Figure S26. *In vivo* tumor growth retardation. Subcutaneous NCR/NU tumor-bearing mice (n = 3) were injected intratumorally (50 µL) with **DOX-M** or PBS; tumor progression was monitored over 25 days with caliper measurements. Data are represented as mean ± SEM; statistical analyses were performed using 2-tailed student t-test (n.s.: not significant, *$p \leq 0.05$, **$p \leq 0.01$, ***$p \leq 0.001$).

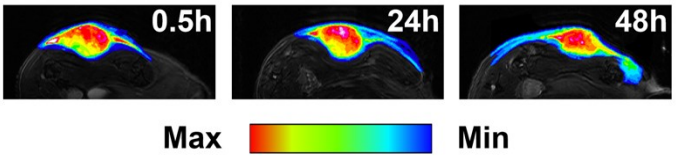

Figure S27. *In vivo* MRI over time of subcutaneous NCR/NU tumor-bearing mice (n = 3) injected intratumorally (50 µL) with non-cleavable BASP-ORCA (**BASP-ORCA1**).[7] False-color inverse-contrast was applied to the tumor for visualization. No significant changes in contrast were observed over the timeframe of the study.

Section B. Materials / General Methods / Instrumentation

All reagents were purchased from commercial suppliers and used without further purification unless otherwise stated. Grubbs 3rd generation bispyridyl catalyst **G3**,[1] macromonomers (MMs) **chex-MM**,[2] **Cy-MM**,[2] **DOX-PC-MM**,[3] **DOX-M-MM**,[4] **yne-MM**,[5] linker **PC-N_3**,[3] **MHC-N_3**,[4] cross-linker **AXL**,[4] payload **chex-NHS**[6] and BASP **BASP-ORCA1**[7] were prepared as previously reported.

Liquid chromatography mass spectrometry (LC/MS) was performed on an Agilent 1260 LC system equipped with a Zorbax SB-C18 rapid resolution HT column using a binary solvent system (MeCN and H_2O with 0.1% CH3COOH). Recycling preparative HPLC was performed on a LaboACE system (Japan Analytical Industry) using a JAIGEL-2 HR JAIGEL-2.5HR column in series. Gel permeation chromatography (GPC) analyses were performed on an Agilent 1260 Infinity setup with two Agilent PL1110-6500 columns in tandem and a 0.025 M LiBr DMF mobile phase run at 60 °C. The differential refractive index (dRI) of each compound was monitored using a Wyatt Optilab T-rEX detector; and, the light scattering (LS) signal was acquired with a Wyatt Dawn Heleos-II detector.

Column chromatography was carried out on silica gel 60F (EMD Millipore, 0.040–0.063 mm) or on aluminum oxide (Sigma-Aldrich, activated, neutral, Brockmann Activity I). Nuclear magnetic resonance (NMR) spectra were recorded on Bruker AVANCE III-400 spectrometer, with working frequencies of 400 (1H), and 100 (13C) MHz, or AVANCE-600 spectrometer with working frequencies of 600 (1H), and 151 (13C) MHz. Chemical shifts are reported in ppm relative to the signals corresponding to the residual non-deuterated solvents: CDCl3: δH = 7.26 ppm and δC = 77.16 ppm. High-resolution mass spectra (HRMS) were measured on a JEOL AccuTOF LC-Plus 4G with an IonSense DART. Matrix-assisted laser desorption/ionization time-of-flight (MALDI-TOF) analyses were collected on a Bruker OmniFlex instrument using sinapinic acid as the matrix. Samples (1 mg) were dissolved in 200 μL acetonitrile; 1 μL of the sample solution was then mixed with 2 μL of the matrix solution, followed by spotting on the sample grid and analysis by MALDI-TOF MS. Electron paramagnetic resonance (EPR) spectra were acquired using a Bruker EMXplus spectrometer. EPR tubes with O. D. 1 mm were used. Typical parameters used for the EPR measurements are modulation frequency: 100 kHz; modulation amplitude: 1 G; time constant: 0.01 ms; conversion time: 5.00 ms; sweep time: 7.50 s; number of scans: 8. The spin concentration reference was 3-carboxy-PROXYL in phosphate-buffered saline or 4-hydroxy-TEMPO in toluene, depending on the samples' solvent. These references were always stored in dry ice, except during measurements, and occasionally re-checked for spin concentration decay.

Dynamic light scattering (DLS) measurements were performed on a Wyatt Technology Mobius DLS instrument. Nanoparticle suspensions were prepared in a solution of nanopure water (MilliQ), PBS buffer,

or 5% v/v glucose/nanopore water (1 mg/mL). The resulting suspensions were passed through a 0.45 μm Nalgene filter (PES membrane) into disposable polystyrene cuvettes, which were pre-cleaned with compressed air. Measurements were made in sets of 10 acquisitions; and, the average hydrodynamic diameters were calculated using the DLS correlation function *via* a regularization fitting method (Dynamics 7.4.0.72 software package from Wyatt Technology).

PC-BASP Release Assay: Stock solutions of **DOX-PC**, **chex-PC**, and **PC1** were prepared in PBS at 5 mg/mL. Aliquots of 100 μL of these solutions were then added to 2 mL LC/MS vials. The vials were then exposed to UV light (VWR UV-AC Dual Hand Lamp, 365 nm) for 0, 5, 10, 15, 20, 30, or 45 min. DMSO (100 μL) were then added to dissolve any insoluble product (none was visible visually). Samples were then analyzed by LC/MS. The resulting free DOX or chex signal was compared against a calibration curve of free DOX or chex to acquire their concentrations; these were then normalized against the theoretical loading of the corresponding BASP, resulting in the normalized release %.

HC-MM Release Assay: Stock solutions of MMs were prepared in PBS at 5 mg/mL. Aliquots of 100 μL of these solutions were then added to 2 mL LC/MS vials. The vials were then incubated at 37°C in an oven. At pre-determined time points, one vial was removed from the oven and allowed to cool down to rt. 100 μL of a standard solution (2 mg/mL 4-bromophenol in DMSO) was then added, and the resulting sample was then analyzed by LC/MS.

In vivo MRI data analysis: Briefly, average signal intensities in regions of interest (ROIs) were acquired for each slide (using ImageJ) and multiplied by the area of the ROI, yielding a total signal for a given slide:

$$ROI\ Signal\ Intensity = Average\ ROI\ Signal\ Intensity \times ROI\ Area$$

This procedure was done for all slides with ROIs, and a volume-averaged signal intensity was obtained:

$$Volumne - averaged\ Signal\ Intensity = Contrast = \frac{\sum ROI\ Signal\ Intensity}{\sum ROI\ Area}$$

The same calculation was done for muscle tissue for normalization purposes, and the normalized signal intensity was acquired via normalization.

$$Normalized\ Contrast = \frac{Tumor\ Contrast}{Muscle\ Contrast}$$

The SNR variations were then acquired, which are the plotted data:

$$SNR\ variation = \frac{Contrast\ at\ time\ t\ post - injection}{Contrast\ at\ t0\ (right\ after\ injection)} \times 100$$

Statistical analysis: BASP diameter acquired by DLS are reported as average ± standard deviation. *In vitro* and *in vivo* signals measured from BASP-ORCAs are reported as mean ± standard error of the mean and plotted with GraphPad Prism (v8.0.2).

Section C. Synthetic Procedures

1. Small Molecule Precursor Synthesis

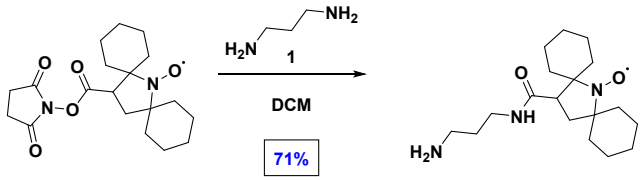

Synthesis of chex-NH$_2$ To a 8 mL vial, **chex-NHS** (212.3 mg, 0.584 mmol, 1.0 eq), and dichloromethane (DCM, 3.5 mL) were added. To another 8 mL vial, 1,3-diaminopropane **1** (433.0 mg, 5.84 mmol, 10.0 eq) was dissolved in DCM (3.5 mL). To the stirring solution of **1**, the **chex-NHS** solution was added dropwise. The reaction mixture was allowed to stir for 3 h at rt. Complete conversion was confirmed by TLC. DCM was then added, and the reaction mixture was washed with water (X2) and brine (X1). The organic layer was collected, dried over Na_2SO_4, filtered, and concentrated under vacuum, affording the product as a yellow solid (134.1 mg, 71% yield, 88.3% spin concentration). HRMS-DART: Calcd for $C_{18}H_{33}N_3O_2$: m/z = 323.2567 $[M + H]^+$; Found: 323.2771. EPR spectrum is provided in **Section C**.

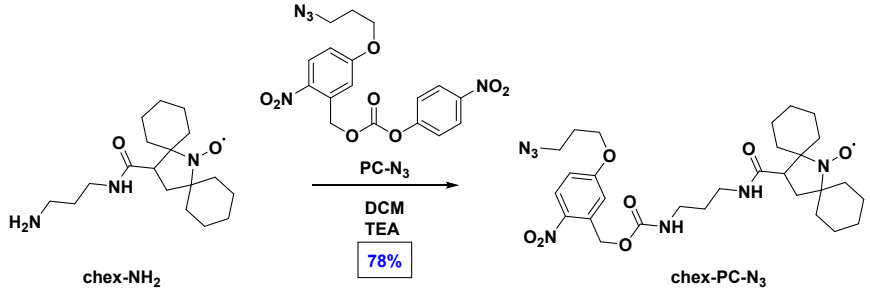

Synthesis of chex-PC-N$_3$ To a 8 mL vial, **chex-NH$_2$** (65.0 mg, 0.201 mmol, 1.15 eq), triethylamine (TEA, 28.4 mg, 39.1 µL, 0.280 mmol, 1.60 eq), and DCM (2 mL) were added. To another 8 mL vial, **PC-N$_3$** (73.2 mg, 0.175 mmol, 1.0 eq) and DCM (2 mL) were added. To the stirring solution of **PC-N$_3$**, the **chex-NH$_2$** solution was added slowly. The reaction was allowed to stir overnight. The crude mixture was concentrated under vacuum, and ran through a silica column (7:1 DCM:ethyl acetate, EtOAc). The fractions containing the product were concentrated under vaccum and dried overnight, affording the pure product as a yellow solid (82.6 mg, 78% yield, 91.2% spin concentration). HRMS-DART: Calcd for $C_{29}H_{43}N_7O_7$: m/z = 601.3218 $[M + H]^+$; Found: 601.3248. EPR spectrum is provided in **Section C**.

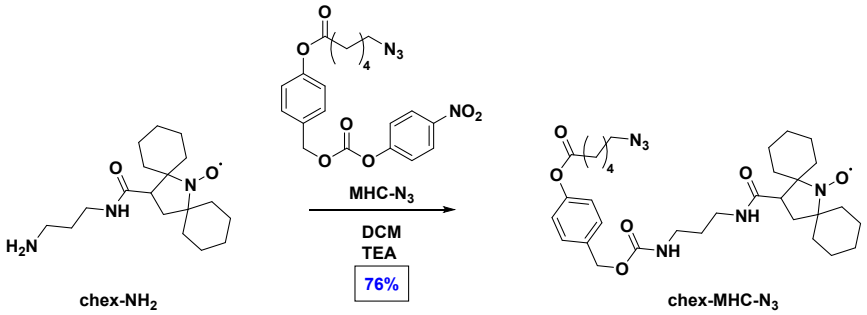

Synthesis of chex-MHC-N$_3$ To a 8 mL vial, **chex-NH$_2$** (45.9 mg, 0.142 mmol, 1.15 eq), TEA (20.0 mg, 27.6 µL, 0.198 mmol, 1.60 eq), and DCM (2 mL) were added. To another 8 mL vial, **MHC-N$_3$** (55.6 mg, 0.124 mmol, 1.0 eq) and DCM (2 mL) were added. To the stirring solution of **MHC-N$_3$**, the **chex-NH$_2$** solution was added slowly. The reaction was allowed to stir overnight. The crude mixture was concentrated under vacuum, and ran through a silica column (7:1 DCM:ethyl acetate, EtOAc). The fractions containing the product were concentrated under vaccum and dried overnight, affording the pure product as a yellow solid (57.5 mg, 76% yield, 92.0% spin concentration). LRMS: Calcd for $C_{32}H_{48}N_6O_6$: m/z = 612.4 $[M + H]^+$; Found: 612.4. EPR spectrum is provided in **Section C**.

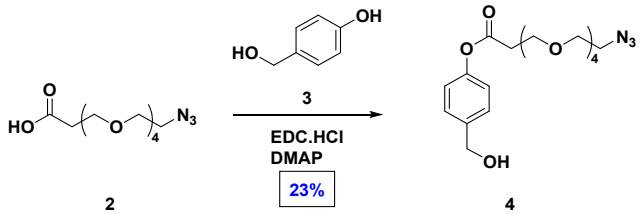

Synthesis of 4 To a 40 mL vial, 4-hydroxybenzyl alcohol **3** (1.5 g, 12.3 mmol, 3.0 eq), *N*-(3-dimethylaminopropyl)-*N*'-ethylcarbodiimide hydrochloride (EDC·HCl, 0.94 g, 4.9 mmol, 1.20 eq), TEA (0.50 g, 0.68 mL, 4.9 mmol, 1.20 eq), 4-dimethylaminopyridine (DMAP, 100.2 mg, 0.82 mmol, 0.20 eq), and chloroform ($CHCl_3$, 8 mL) were added, which was then cooled in an ice bath. To a 4 mL vial, azido-PEG4-acid **2** (1.2 g, 4.1 mmol, 1.00 eq) and $CHCl_3$ (2 mL) were added. To the stirring solution of **3**, the **2** solution was added dropwise. The reaction was allowed to warm to rt and stirred for 4 h. The reaction mixture was concentrated under vacuum, redissolved in $CHCl_3$, filtered through a 0.45 µm filter (Nalgene), and subjected to recycling preparative HPLC. The fractions containing the product were concentrated under vaccum and dried overnight, affording the pure product as a clear liquid (361.2 mg, 23% yield). HRMS-DART: Calcd for $C_{18}H_{28}N_3O_7$: m/z = 398.1922 $[M + H]^+$; Found: 398.2134. ^{1}H NMR (400 MHz, $CDCl_3$) δ 7.37 (d, *J* = 8.5 Hz, 2H), 7.07 (d, *J* = 8.5 Hz, 2H), 4.67 (s, 2H), 3.86 (t, *J* = 6.3 Hz, 2H), 3.66 (m, 14H), 3.37 (t, *J* = 5.1 Hz, 2H), 2.83 (t, *J* = 6.3 Hz, 2H). ^{13}C NMR (126 MHz, $CDCl_3$) δ 170.33, 150.15, 138.69, 128.15, 121.79, 70.81, 70.80, 70.76, 70.68, 70.66, 70.14, 66.61, 64.83, 50.80, 35.38, 28.22.

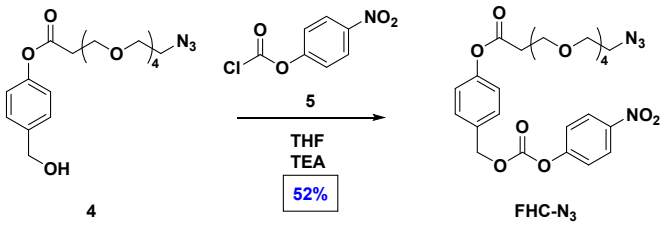

Synthesis of FHC-N₃ To a 8 mL vial, **4** (250.0 mg, 0.629 mmol, 1.0 eq), TEA (89.1 mg, 0.123 mL, 0.881 mmol, 1.40 eq), and tetrahydrofuran (THF, 4 mL) were added. To a 40 mL vial, 4-nitrophenyl chloroformate **5** (240.9 mg, 1.195 mmol, 1.90 eq) and THF (7.5 mL) were added, which was then cooled in an ice bath. To the stirring solution of **5**, the **4** solution was added dropwise. The reaction was allowed to warm to rt and stirred for 1 h. The reaction mixture was concentrated under vacuum, redissolved in $CHCl_3$, filtered through a 0.45 µm filter (Nalgene), and subjected to recycling preparative HPLC. The fractions containing the product were concentrated under vaccum and dried overnight, affording the pure product as a clear liquid (184.7 mg, 52% yield). HRMS-DART: Calcd for $C_{25}H_{31}N_4O_{11}$: m/z = 563.1984 $[M + H]^+$; Found: 563.2002. ^{1}H NMR (400 MHz, $CDCl_3$) δ 8.27 (d, *J* = 9.1 Hz, 2H), 7.46 (d, *J* = 8.5 Hz, 2H), 7.37 (d, *J* = 9.1 Hz, 2H), 7.14 (d, *J* = 8.5 Hz, 2H), 5.27 (s, 2H), 3.87 (t, *J* = 6.3 Hz, 2H), 3.66 (m, 14H), 3.37 (t, *J* = 5.1 Hz, 2H), 2.85 (t, *J* = 6.3 Hz, 2H). ^{13}C NMR (126 MHz, $CDCl_3$) δ 170.14, 155.59, 152.51, 151.28, 145.54, 131.90, 130.14, 125.42, 122.16, 121.90, 70.81, 70.80, 70.75, 70.68, 70.65, 70.38, 70.14, 66.54, 50.79, 35.37.

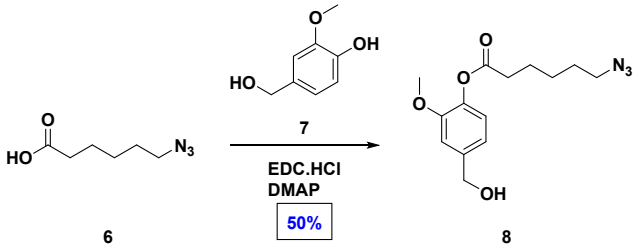

Synthesis of 8 To a 100 mL flask, 4-hydroxy-3-methoxybenzyl alcohol **7** (4.47 g, 0.029 mol, 3.0 eq), EDC·HCl (2.18 g, 11.4 mmol, 1.20 eq), TEA (1.15 g, 1.59 mL, 11.4 mmol, 1.20 eq), DMAP (0.23 g, 1.9 mmol, 0.20 eq), and DCM (30 mL) were added, which was then cooled in an ice bath. To a 40 mL vial, 6-azido hexanoic acid **6** (1.2 g, 4.1 mmol, 1.00 eq) and DCM (10 mL) were added. To the stirring solution of **7**, **6** was added dropwise. The reaction was allowed to warm to rt and stirred overnight. The reaction mixture was concentrated under vacuum, redissolved in $CHCl_3$, filtered through a 0.45 µm filter (Nalgene), and subjected to recycling preparative HPLC. The fractions containing the product were concentrated under vaccum and dried overnight, affording the pure product as a clear liquid (1.46 g, 50% yield). HRMS-DART: Calcd for $C_{14}H_{20}N_3O_4$: m/z = 294.1448 $[M + H]^+$; Found: 294.1447. ^{1}H NMR (400 MHz, $CDCl_3$) δ 7.16 – 6.61 (m, 3H), 4.66 (s, 2H), 3.83 (s, 3H), 3.30 (t, *J* = 6.8 Hz, 2H), 2.60 (t, *J* = 7.4

Hz, 2H), 1.80 (m, 2H), 1.67 (m, 2H), 1.58 – 1.46 (m, 2H). ^{13}C NMR (126 MHz, $CDCl_3$) δ 171.72, 151.29, 140.02, 139.18, 122.81, 119.09, 111.13, 65.15, 55.97, 51.40, 33.91, 28.69, 26.28, 24.63.

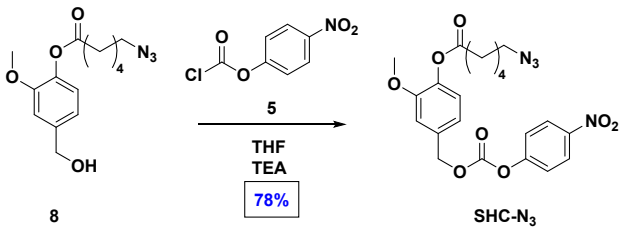

Synthesis of SHC-N$_3$ To a 40 mL vial, **8** (450.0 mg, 1.534 mmol, 1.0 eq), TEA (217.3 mg, 0.299 mL, 2.148 mmol, 1.40 eq), and THF (7 mL) were added. To another 40 mL vial, 4-nitrophenyl chloroformate **5** (587.5 mg, 2.915 mmol, 1.90 eq) and THF (18 mL) were added, which was then cooled in an ice bath. To the stirring solution of **5**, the **8** solution was added dropwise. The reaction was allowed to warm to rt and stirred for 1 h. The reaction mixture was concentrated under vacuum, redissolved in $CHCl_3$, filtered through a 0.45 µm filter (Nalgene), and subjected to recycling preparative HPLC. The fractions containing the product were concentrated under vaccum and dried overnight, affording the pure product as a clear liquid (551.2 mg, 78% yield). LRMS: Calcd for $C_{21}H_{23}N_4O_8$: m/z = 459.2 $[M + H]^+$; Found: 459.1. ^{1}H NMR (500 MHz, $CDCl_3$) δ 8.28 (d, *J* = 9.2 Hz, 2H), 7.39 (d, *J* = 9.2 Hz, 2H), 7.11 – 6.97 (m, 3H), 5.27 (s, 2H), 3.86 (s, 3H), 3.31 (t, *J* = 6.8 Hz, 2H), 2.61 (t, *J* = 7.4 Hz, 2H), 1.88 – 1.76 (m, 2H), 1.73 – 1.62 (m, 2H), 1.57 – 1.41 (m, 2H). ^{13}C NMR (126 MHz, $CDCl_3$) δ 171.50, 155.62, 152.57, 151.47, 145.60, 140.48, 133.09, 125.47, 123.24, 121.94, 121.40, 112.96, 70.75, 56.09, 51.42, 33.91, 28.71, 26.30, 24.62.

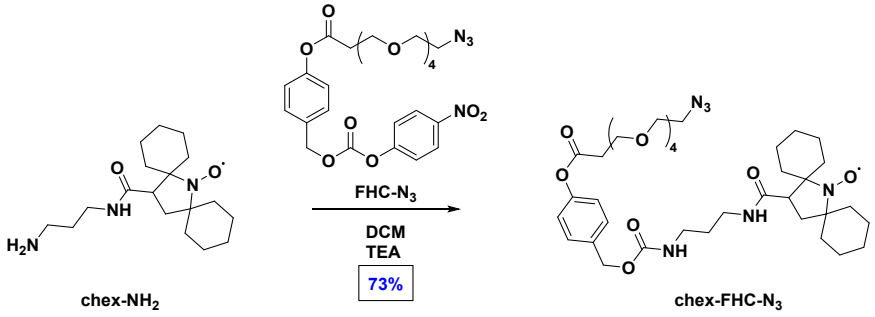

Synthesis of chex-FHC-N$_3$ To a 8 mL vial, **chex-NH$_2$** (50.0 mg, 0.155 mmol, 1.15 eq), TEA (21.8 mg, 30.1 µL, 0.216 mmol, 1.60 eq), and DCM (2 mL) were added. To another 8 mL vial, **FHC-N$_3$** (75.9 mg, 0.135 mmol, 1.0 eq) and DCM (2 mL) were added. To the stirring solution of **FHC-N$_3$**, the **chex-NH$_2$** solution was added slowly. The reaction was allowed to stir overnight. The reaction mixture was concentrated under vacuum, redissolved in $CHCl_3$, filtered through a 0.45 µm filter (Nalgene), and subjected to recycling preparative HPLC. The fractions containing the product were concentrated under vaccum and dried overnight, affording the pure product as a yellow solid (75.3 mg, 73% yield, 95.1%

spin concentration). LRMS: Calcd for $C_{37}H_{57}KN_6O_{10}$: m/z = 784.4 $[M + K]^+$; Found: 784.4. EPR spectrum is provided in **Section C**.

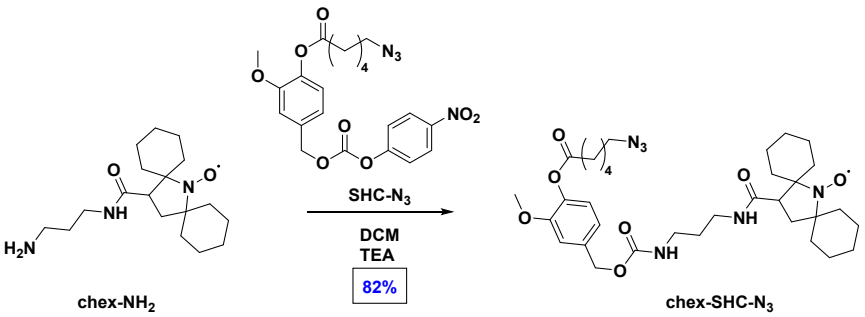

Synthesis of chex-SHC-N$_3$ To a 8 mL vial, **chex-NH$_2$** (61.0 mg, 0.189 mmol, 1.15 eq), TEA (26.6 mg, 36.0 µL, 0.263 mmol, 1.60 eq), and DCM (2.5 mL) were added. To another 8 mL vial, **SHC-N$_3$** (75.4 mg, 0.164 mmol, 1.0 eq) and DCM (2.5 mL) were added. To the stirring solution of **SHC-N$_3$**, the **chex-NH$_2$** solution was added slowly. The reaction was allowed to stir overnight. The reaction mixture was concentrated under vacuum, redissolved in $CHCl_3$, filtered through a 0.45 µm filter (Nalgene), and subjected to recycling preparative HPLC. The fractions containing the product were concentrated under vaccum and dried overnight, affording the pure product as a yellow solid (88.0 mg, 82% yield, 96.3% spin concentration). HRMS-DART: Calcd for $C_{33}H_{50}N_6O_7$: m/z = 642.3735 $[M + H]^+$; Found: 642.3773. EPR spectrum is provided in **Section C**.

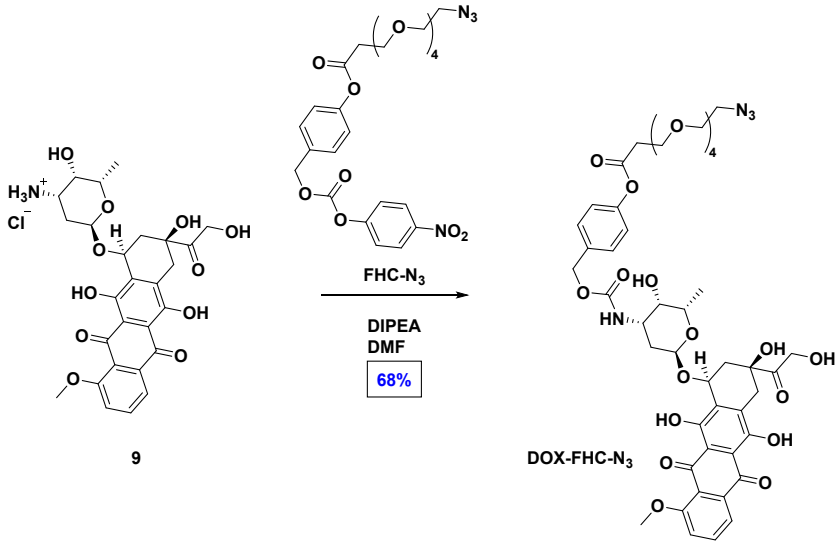

Synthesis of DOX-FHC-N$_3$ To a 8 mL vial, doxorubicin hydrochloride **9** (55.2 mg, 0.095 mmol, 1.07 eq), **FHC-N$_3$** (50.0 mg, 0.089 mmol, 1.0 eq), N,N-Diisopropylethylamine (DIPEA, 12.3 mg, 16.6 µL, 0.095 mmol, 1.07 eq), and dimethyl formamide (DMF, 3.0 mL) were added. The reaction mixture was allowed to stir overnight at rt. EtOAc was then added, and the reaction mixture was washed with water (X2) and brine (X1). The organic layer was collected, dried over Na_2SO_4, filtered, and concentrated under vacuum.

The crude mixture was ran through a silica column (0 → 10% methanol, MeOH, in DCM). The fractions containing the product were concentrated under vaccum and dried overnight, affording the pure product as a red solid (58.0 mg, 68% yield) . MALDI-TOF MS: Calcd for $C_{46}H_{54}NaN_4O_{19}$: m/z = 989.327 [M + Na]$^+$; Found: 989.386. ^{1}H NMR (400 MHz, $CDCl_3$) δ 13.98 (s, 1H), 13.26 (s, 1H), 8.04 (d, *J* = 6.5 Hz, 1H), 7.79 (t, *J* = 8.2 Hz, 1H), 7.40 (d, *J* = 9.0 Hz, 1H), 7.32 (d, J = 8.1 Hz, 2H), 7.17 – 6.83 (m, 2H), 5.50 (s, 1H), 5.29 (s, 1H), 5.13 (d, *J* = 8.5 Hz, 1H), 5.01 (s, 2H), 4.76 (s, 2H), 4.54 (s, 1H), 4.21 – 4.03 (m, 4H), 3.84 (m, 3H), 3.65 (s, 14H), 3.37 (s, 2H), 3.28 (d, *J* = 18.9 Hz, 1H), 3.15 – 2.95 (m, 2H), 2.82 (s, 2H), 2.33 (d, *J* = 14.7 Hz, 1H), 2.17 (d, *J* = 14.7 Hz, 1H), 2.03 – 1.91 (m, 1H), 1.87 (m, 1H), 1.78 (m, 1H), 1.28 (s, 3H). ^{13}C NMR (126 MHz, $CDCl_3$) δ 213.99, 187.22, 186.83, 170.20, 161.19, 156.31, 155.78, 155.55, 150.56, 135.91, 135.63, 134.12, 133.72, 133.69, 129.50, 121.79, 121.00, 119.98, 118.60, 111.72, 111.56, 100.85, 76.75, 70.81, 70.79, 70.76, 70.67, 70.65, 70.15, 69.79, 69.65, 67.40, 66.58, 66.22, 65.68, 56.81, 50.81, 47.13, 35.76, 35.35, 34.14, 30.28, 16.97.

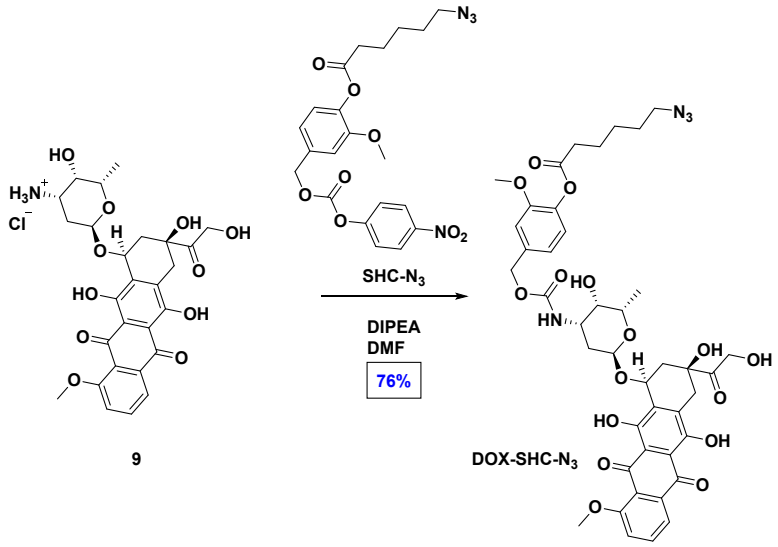

Synthesis of DOX-SHC-N$_3$ To a 8 mL vial, doxorubicin hydrochloride **9** (67.7 mg, 0.117 mmol, 1.07 eq), **SHC-N$_3$** (50.0 mg, 0.109 mmol, 1.0 eq), DIPEA (15.1 mg, 20.3 µL, 0.117 mmol, 1.07 eq), and DMF (1.75 mL) were added. The reaction mixture was allowed to stir overnight at rt. EtOAc was then added, and the reaction mixture was washed with water (X2) and brine (X1). The organic layer was collected, dried over Na_2SO_4, filtered, and concentrated under vacuum. The crude mixture was ran through a silica column (0 → 10% MeOH in DCM). The fractions containing the product was concentrated under vaccum and dried overnight, affording the pure product as a red solid (71.7 mg, 76% yield). LRMS: Calcd for $C_{42}H_{46}KN_4O_{16}$: m/z = 901.3 [M + K]$^+$; Found: 901.1. 1H NMR (500 MHz, $CDCl_3$) δ 13.98 (s, 1H), 13.25 (s, 1H), 8.04 (d, *J* = 7.8 Hz, 1H), 7.88 – 7.69 (t, *J* = 8.1 Hz, 1H), 7.39 (d, *J* = 8.6 Hz, 1H), 7.02 – 6.80 (m, 3H), 5.51 (d, *J* = 4.0 Hz, 1H), 5.30 (s, 1H), 5.13 (d, *J* = 8.7 Hz, 1H), 5.00 (s, 2H), 4.76 (s, 2H), 4.54 (s, 1H), 4.14 (d, *J* = 6.7 Hz, 1H), 4.08 (s, 3H), 3.79 (m, 4H), 3.67 (s, 1H), 3.31-3.26 (m, 3H), 3.05 (s, 1H),

3.01 (s, 1H), 2.57 (t, *J* = 7.4 Hz, 2H), 2.33 (d, *J* = 14.7 Hz, 1H), 2.17 (dd, *J* = 14.7, 4.1 Hz, 1H), 1.89 (dd, *J* = 13.5, 5.1 Hz, 2H), 1.84 – 1.73 (m, 3H), 1.69 – 1.61 (m, 2H), 1.58 – 1.46 (m, 2H), 1.29 (d, *J* = 6.6 Hz, 3H).^{13}C NMR (126 MHz, $CDCl_3$) δ 213.97, 187.29, 186.89, 171.56, 161.23, 156.33, 155.82, 155.52, 151.18, 139.69, 135.94, 135.68, 135.32, 133.73, 133.67, 122.88, 121.06, 120.70, 120.02, 118.60, 112.46, 111.78, 111.60, 100.84, 76.78, 69.83, 69.70, 67.39, 66.60, 65.70, 56.84, 56.02, 51.41, 47.16, 35.79, 34.19, 33.89, 30.32, 28.69, 26.28, 24.61, 16.98.

2. Macromomer Synthesis

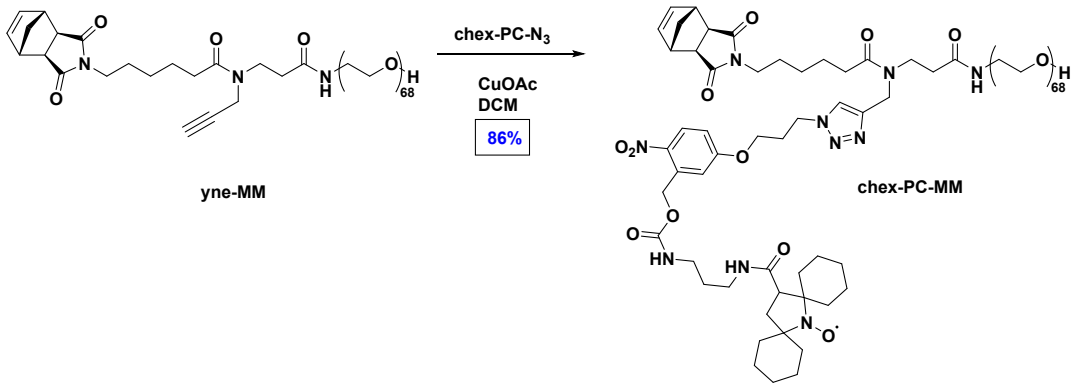

Synthesis of chex-PC-MM To a vial, **yne-MM** (117.7 mg, 0.035 mmol, 1.0 eq), **chex-PC-N_3** (25.0 mg, 0.041 mmol, 1.17 eq), and DCM (4.0 mL) were added. Copper(I) acetate (CuOAc) (a pinch) was then added and the reaction mixture was stirred under N_2 atmosphere. The reaction was complete in ~1 h as determined by LC-MS. The crude mixture was ran through an aluminum oxide plug. The collected solution was concentrated under vacuum, redissolved in $CHCl_3$, filtered through a 0.45 μm filter (Nalgene), and subjected to recycling preparative HPLC. The fractions containing the product were concentrated under vaccum and dried overnight, affording the pure product as an off-white solid (119.6 mg, 86% yield, 91.3% spin concentration). EPR and MALDI-TOF spectra are provided in **Section C.**

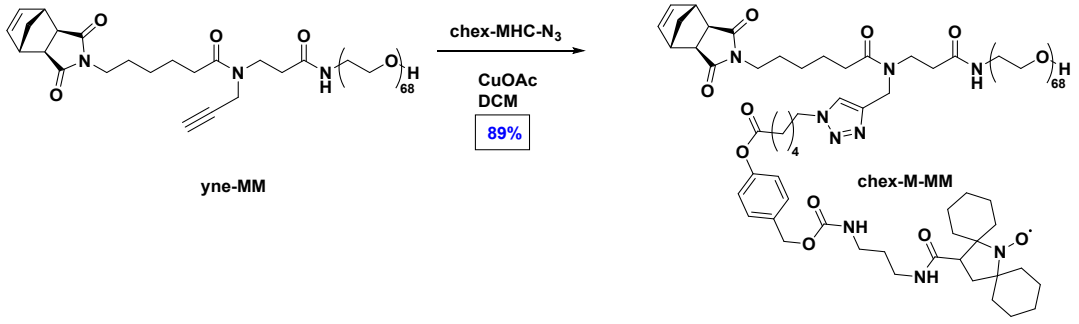

Synthesis of chex-M-MM To a vial, **yne-MM** (229.4 mg, 0.068 mmol, 1.0 eq), **chex-MHC-N_3** (50.0 mg, 0.082 mmol, 1.2 eq), and DCM (9.0 mL) were added. CuOAc (a pinch) was then added and the reaction mixture was stirred under N_2 atmosphere. The reaction was complete in ~1 h as determined by LC-MS. The crude mixture was ran through an aluminum oxide plug. The collected solution was concentrated under vacuum, redissolved in $CHCl_3$, filtered through a 0.45 μm filter (Nalgene), and subjected to recycling preparative HPLC. The fractions containing the product were concentrated under vaccum and dried overnight, affording the pure product as an off-white solid (241.8 mg, 89% yield, 92.1% spin concentration). EPR and MALDI-TOF spectra are provided in **Section C.**

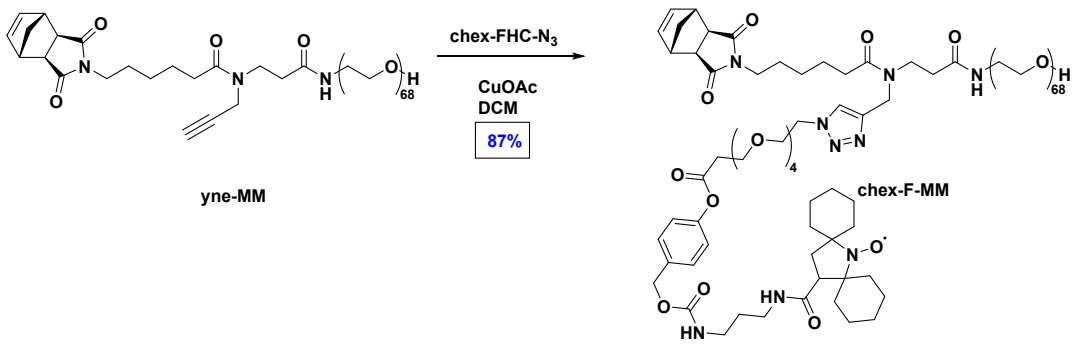

Synthesis of chex-F-MM To a vial, **yne-MM** (158.0 mg, 0.047 mmol, 1.0 eq), **chex-FHC-N_3** (41.0 mg, 0.054 mmol, 1.15 eq), and DCM (6.0 mL) were added. CuOAc (a pinch) was then added and the reaction mixture was stirred under N_2 atmosphere. The reaction was complete in ~1 h as determined by LC-MS. The crude mixture was ran through an aluminum oxide plug. The collected solution was concentrated under vacuum, redissolved in $CHCl_3$, filtered through a 0.45 μm filter (Nalgene), and subjected to recycling preparative HPLC. The fractions containing the product were concentrated under vaccum and dried overnight, affording the pure product as an off-white solid (167.9 mg, 87% yield, 89.6% spin concentration). EPR and MALDI-TOF spectra are provided in **Section C.**

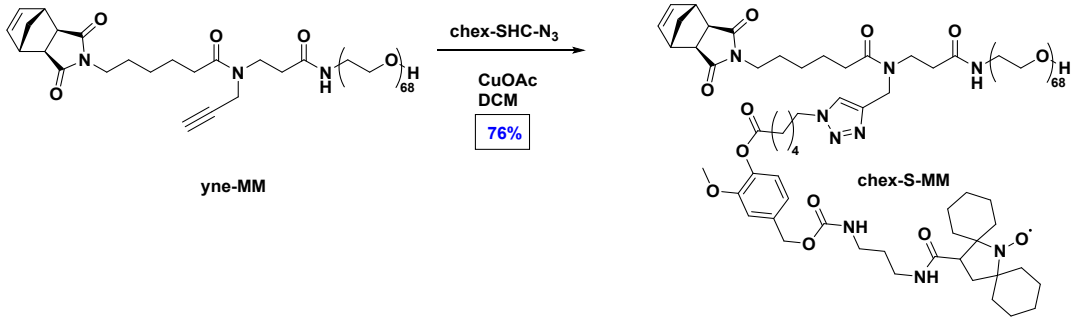

Synthesis of chex-S-MM To a vial, **yne-MM** (193.8 mg, 0.058 mmol, 1.0 eq), **chex-SHC-N_3** (43.4 mg, 0.066 mmol, 1.15 eq), and DCM (7.0 mL) were added. CuOAc (a pinch) was then added and the reaction mixture was stirred under N_2 atmosphere. The crude mixture was ran through an aluminum oxide plug. The collected solution was concentrated under vacuum, redissolved in $CHCl_3$, filtered through a 0.45 μm filter (Nalgene), and subjected to recycling preparative HPLC. The fractions containing the product were concentrated under vaccum and dried overnight, affording the pure product as an off-white solid (174.9 mg, 76% yield, 92.1% spin concentration). EPR and MALDI-TOF spectra are provided in **Section C.**

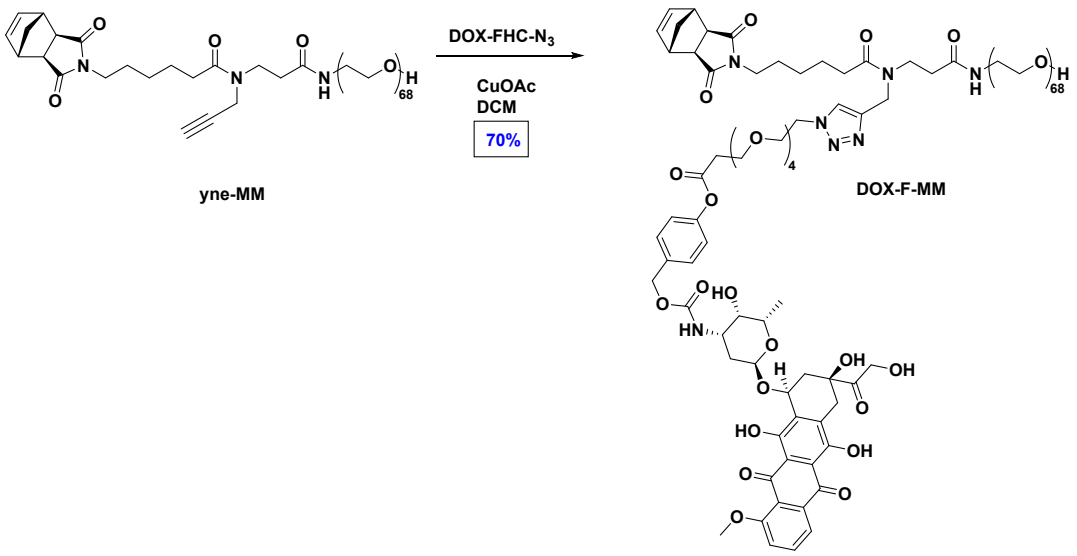

Synthesis of DOX-F-MM To a vial, **yne-MM** (88.1 mg, 0.026 mmol, 1.0 eq), **DOX-FHC-N_3** (30.0 mg, 0.030 mmol, 1.15 eq), and DCM (4.0 mL) were added. CuOAc (a pinch) was then added and the reaction mixture was stirred under N_2 atmosphere. The crude mixture was ran through an aluminum oxide plug. The collected solution was concentrated under vacuum, redissolved in $CHCl_3$, filtered through a 0.45 µm filter (Nalgene), and subjected to recycling preparative HPLC. The fractions containing the product were concentrated under vaccum and dried overnight, affording the pure product as a red solid (80.4 mg, 70% yield). ^{1}H NMR and MALDI-TOF spectra are provided in **Section C.**

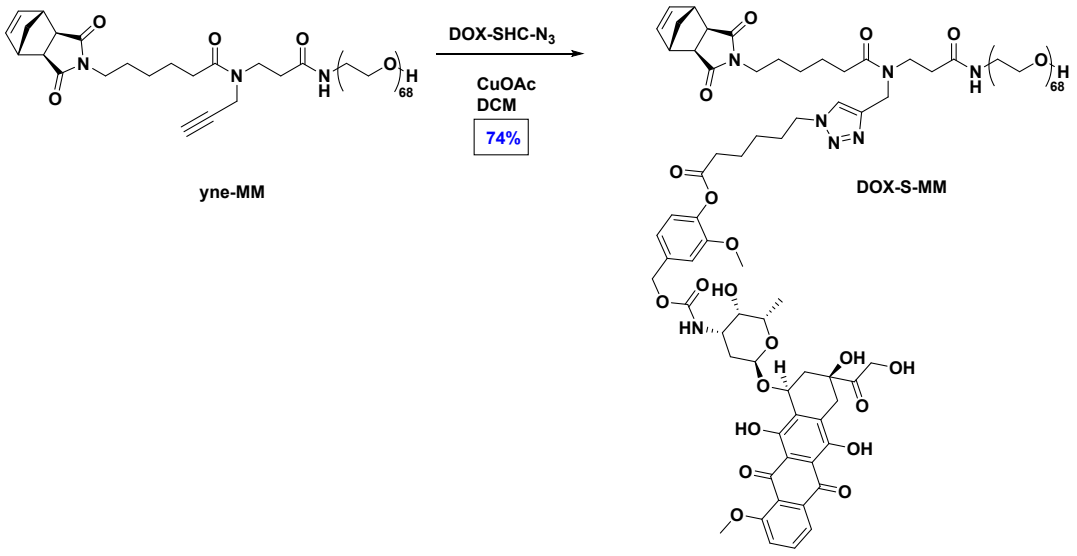

Synthesis of DOX-S-MM To a vial, **yne-MM** (64.5 mg, 0.019 mmol, 1.0 eq), **DOX-SHC-N_3** (19.0 mg, 0.022 mmol, 1.15 eq), and DCM (4.0 mL) were added. CuOAc (a pinch) was then added and the reaction mixture was stirred under N_2 atmosphere. The crude mixture was ran through an aluminum oxide plug. The collected solution was concentrated under vacuum, redissolved in $CHCl_3$, filtered through a 0.45 µm filter (Nalgene), and subjected to recycling preparative HPLC. The fractions containing the product were

concentrated under vaccum and dried overnight, affording the pure product as a red solid (59.6 mg, 74% yield). ^{1}H NMR and MALDI-TOF spectra are provided in **Section C.**

3. Brush-Arm Star Polymer (BASP) Synthesis.

Note: *All BASP syntheses were performed in a glovebox under N_2 atmosphere; however, similar results are expected under ambient conditions. All ROMP reactions followed the same general procedure, which was modified from literature examples.*[3,4,7]

Chemical structure of BASP building blocks

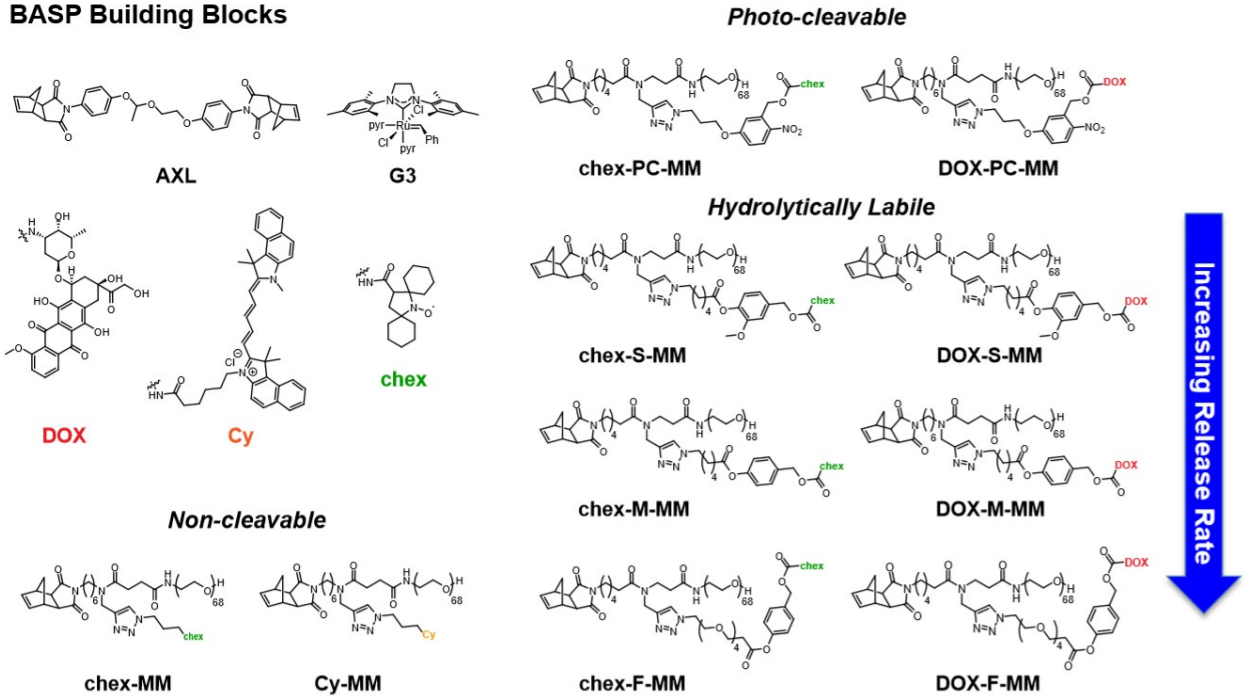

*Representative procedure for BASP (**S**) synthesis with brush length of 7.07 (m) and 20 equivalents (N) of cross-linker (**S**, m=7.07—6/1/0.07 chex/DOX/Cy; N=20):* To a 4 mL vial, a suspension of **AXL** (18.2 mg, 31.4 µmol, 20.0 eq) in THF (313.9 µL, 0.1 M **AXL**) was prepared. To a second 4 mL vial containing a stir bar, **chex-S-MM** (37.9 mg, 9.4 µmol, 6.0 eq) was added; **DOX-S-MM** was then added from a premade 50 mg/mL solution in THF (132.8 µL, 1.6 µmol, 1.0 eq); **Cy-MM** was then added from a premade 12.5 mg/mL solution in THF (35.9 µL, 0.11 µmol, 0.07 eq). To a third vial, a solution of Grubbs 3rd generation bispyridyl catalyst (**G3**, 0.02 M in THF) was freshly prepared. THF (10.6 µL) was then added to the MM vial, followed by the addition of Grubbs 3rd solution (78.5 µL, 1.6 µmol, 1.0 eq) to give the desired MM:G3-cat ratio of 7.07:1 (1 mol % of the **Cy-MM**), while achieving a total MM concentration of 0.05 M, affording a dark brown solution. The reaction mixture was allowed to stir for 30 min at room temperature before an aliquot (~5 µL) was taken out and quenched with 1 drop of ethyl vinyl ether for GPC analysis. The **AXL** suspension was then added dropwise (in aliquots of 5 eq, or ~80 µL, every 5 min) over the course of 20 min into the MM vial, and the polymerizing mixture was allowed to stir for 6 h at room temperature, affording a dark brown solution. To quench the polymerization, a drop of

ethyl vinyl ether was added. The reaction mixture was transferred to an 8 kD molecular weight cutoff dialysis tubing (Spectrum Laboratories) in 5 mL nanopure water, and the solution was dialyzed against H_2O (500 mL × 3, solvent exchange every 6 h). The dialyzed solution of **S** was then concentrated to the desired concentration via centrifugation with a filter tube (30 kDa MWCO, Millipore Sigma). Other BASPs compositions were prepared following similar procedures with the corresponding MMs and stoichiometry.

Section D. Spectral Data of Small Molecule Precursors

Spectra Data for chex-NH_2, chex-PC-N_3, chex-MHC-N_3

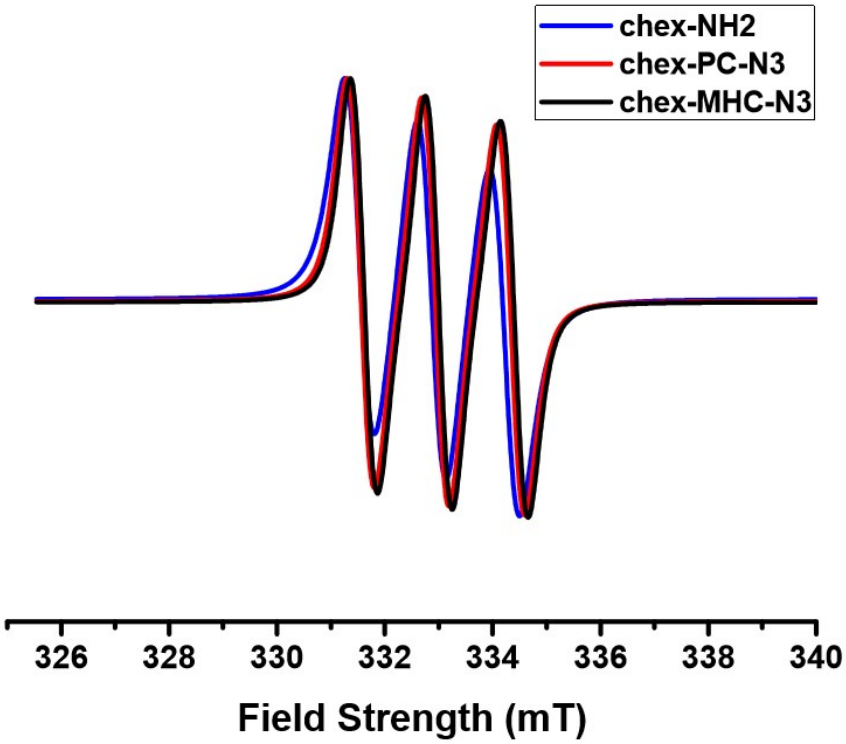

Figure S28. EPR Spectra of **chex-NH$_2$**, **chex-PC-N$_3$**, and **chex-MHC-N$_3$**

Spectra Data for 4

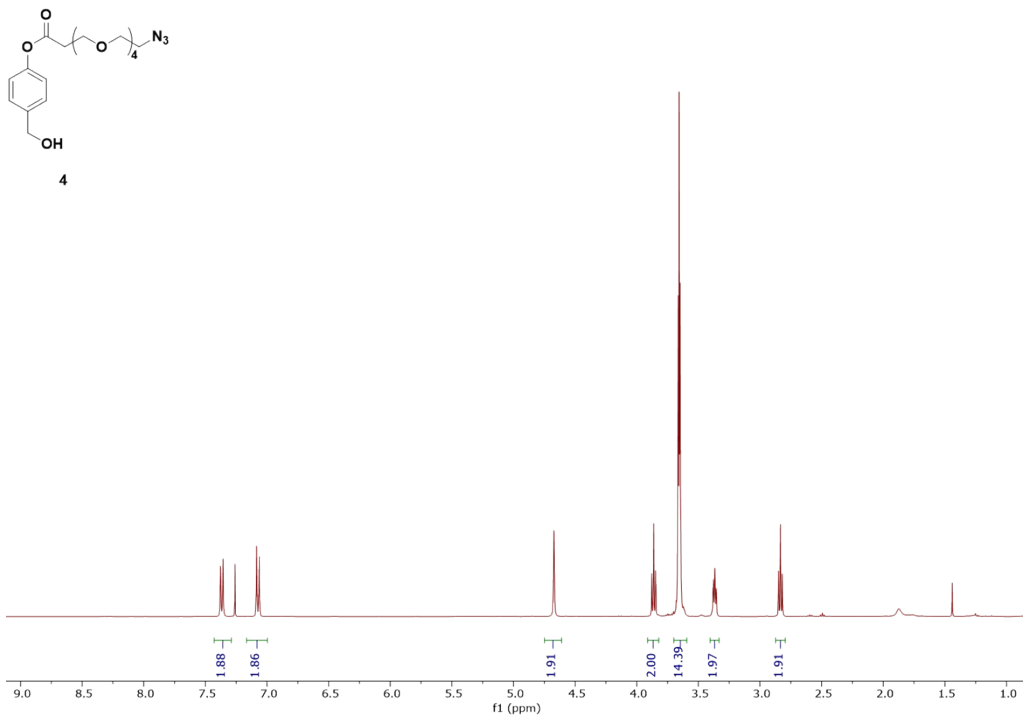

Figure S29. ^{1}H NMR Spectrum of **4** in $CDCl_3$

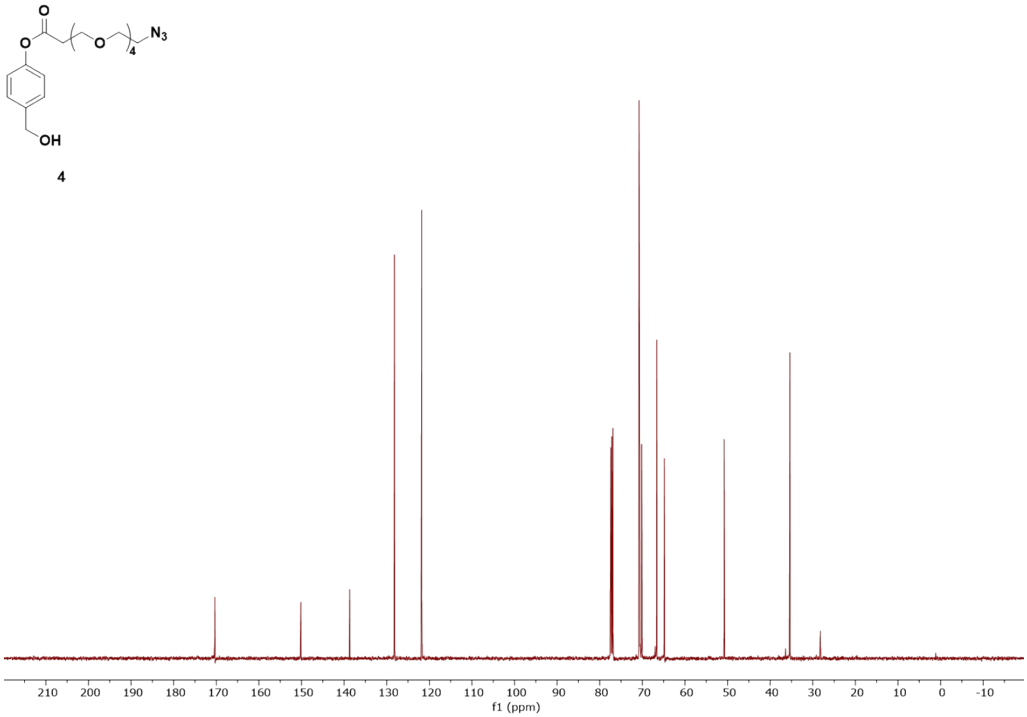

Figure S30. ^{13}C NMR Spectrum of **4** in $CDCl_3$

Spectra Data for FHC-N_3

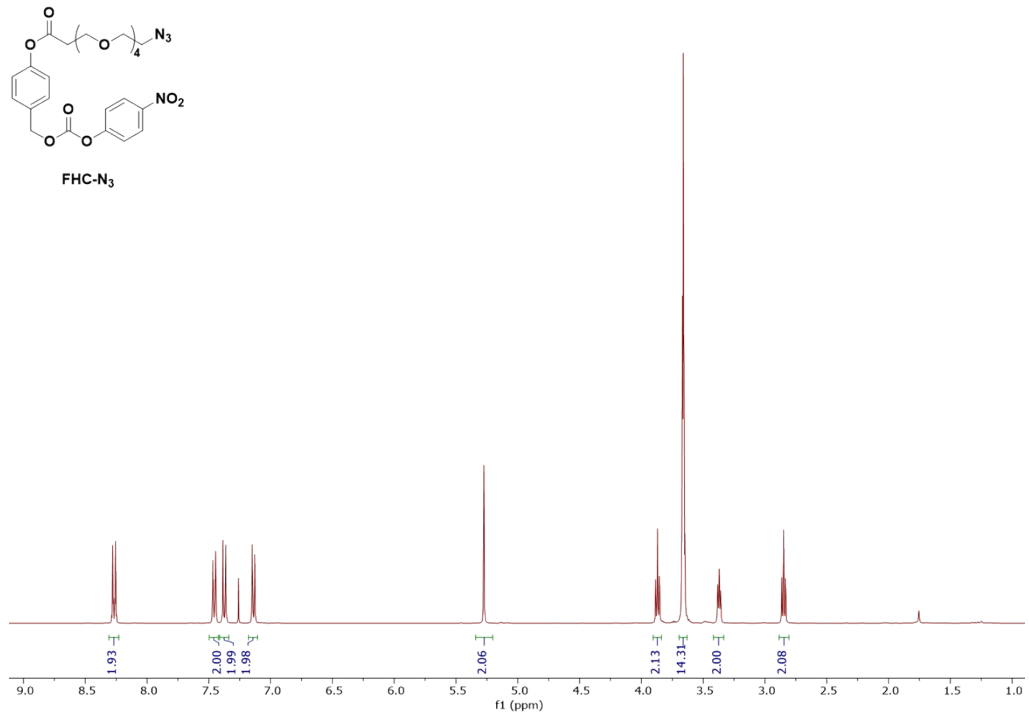

Figure S31. ^{1}H NMR Spectrum of **FHC-N_3** in $CDCl_3$

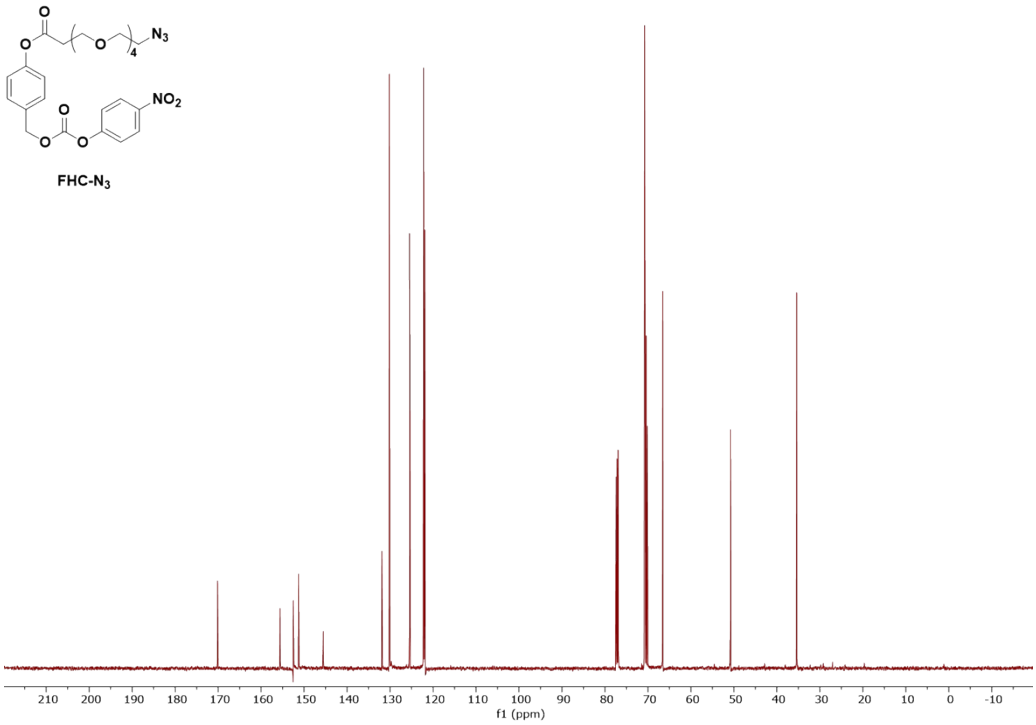

Figure S32. ^{13}C NMR Spectrum of **FHC-N_3** in $CDCl_3$

Spectra Data for 8

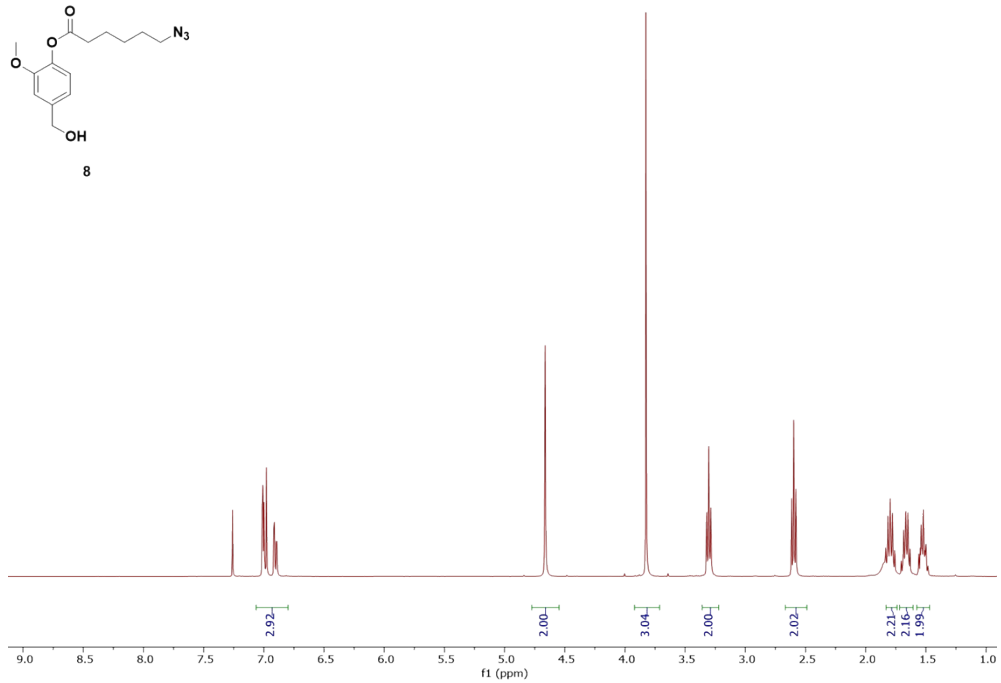

Figure S33. ^{1}H NMR Spectrum of **8** in $CDCl_3$

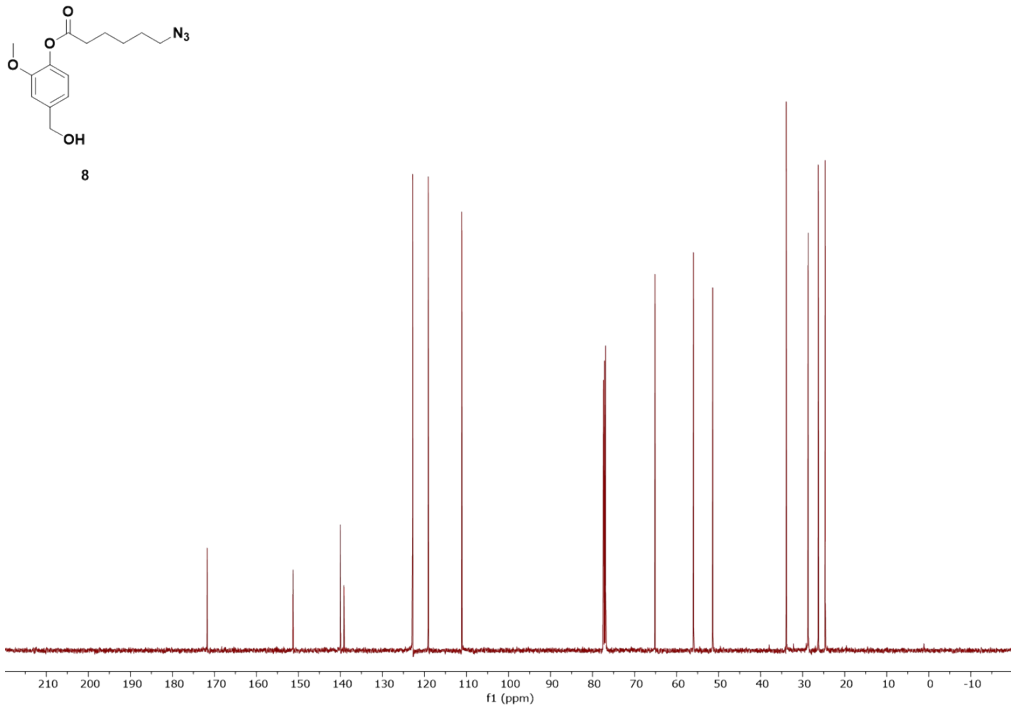

Figure S34. ^{13}C NMR Spectrum of **8** in $CDCl_3$

Spectra Data for SHC-N_3

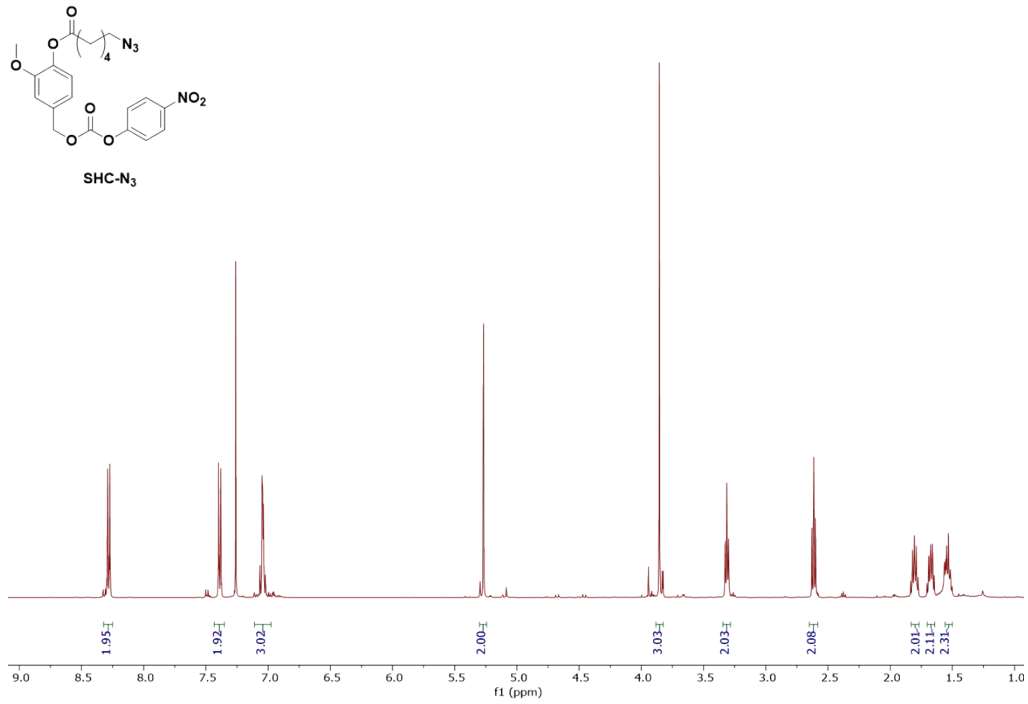

Figure S35. ^{1}H NMR Spectrum of **SHC-N_3** in $CDCl_3$

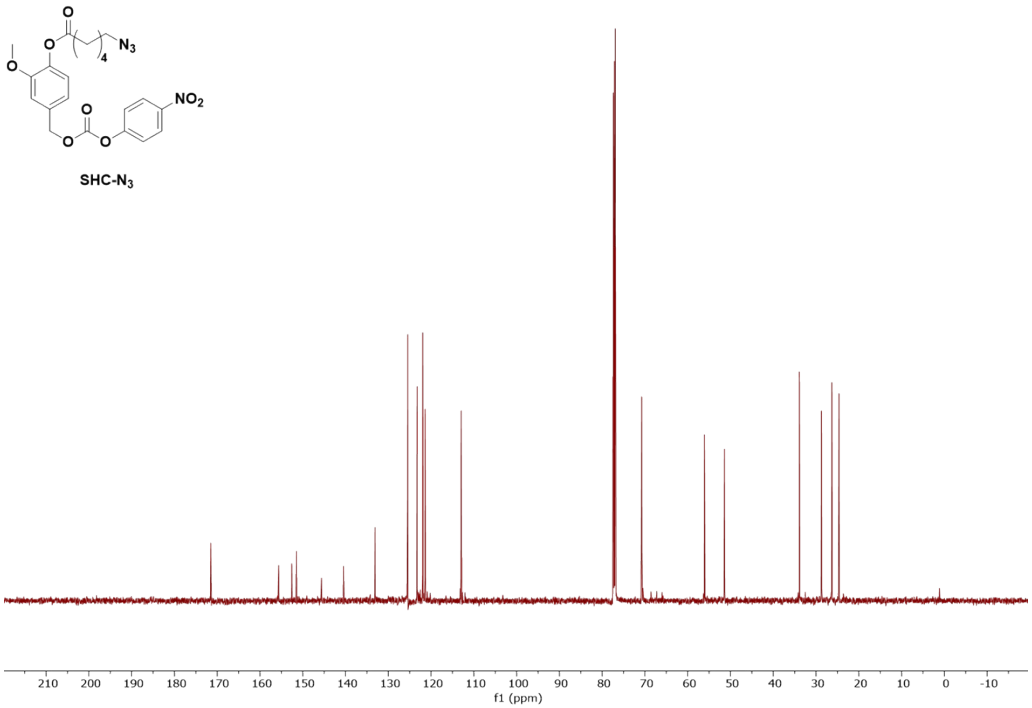

Figure S36. ^{13}C NMR Spectrum of **SHC-N_3** in $CDCl_3$

Spectra Data for chex-FHC-N_3, chex-SHC-N_3

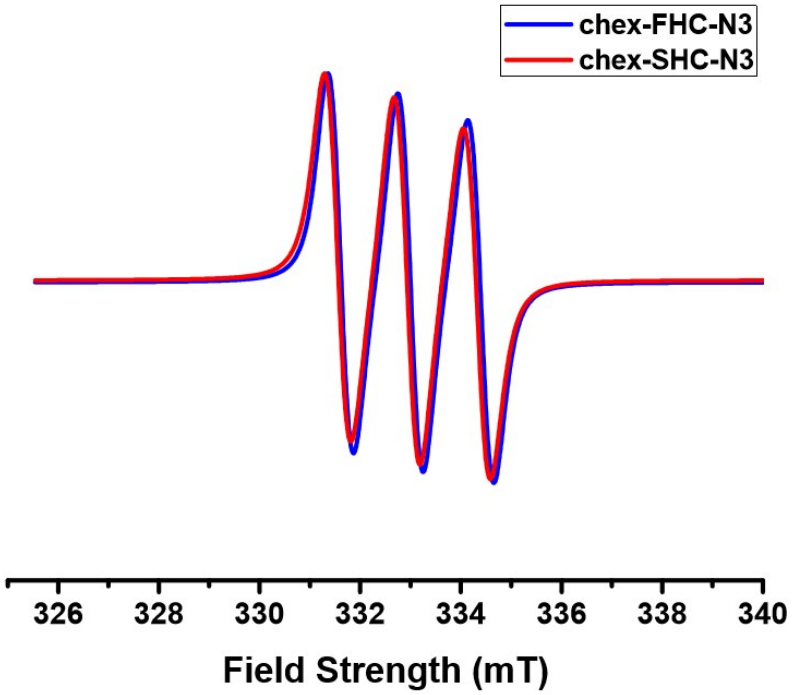

Figure S37. EPR Spectra of **chex-FHC-N_3**, and **chex-FHC-N_3**

Spectra Data for DOX-FHC-N_3

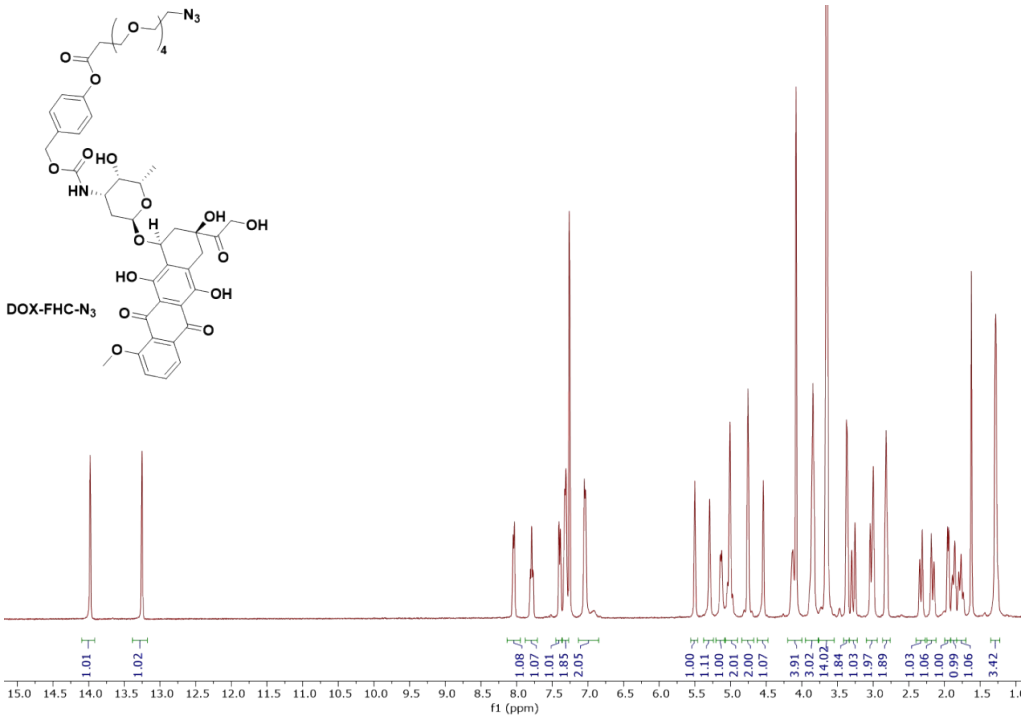

Figure S38. ^{1}H NMR Spectrum of **DOX-FHC-N_3** in $CDCl_3$

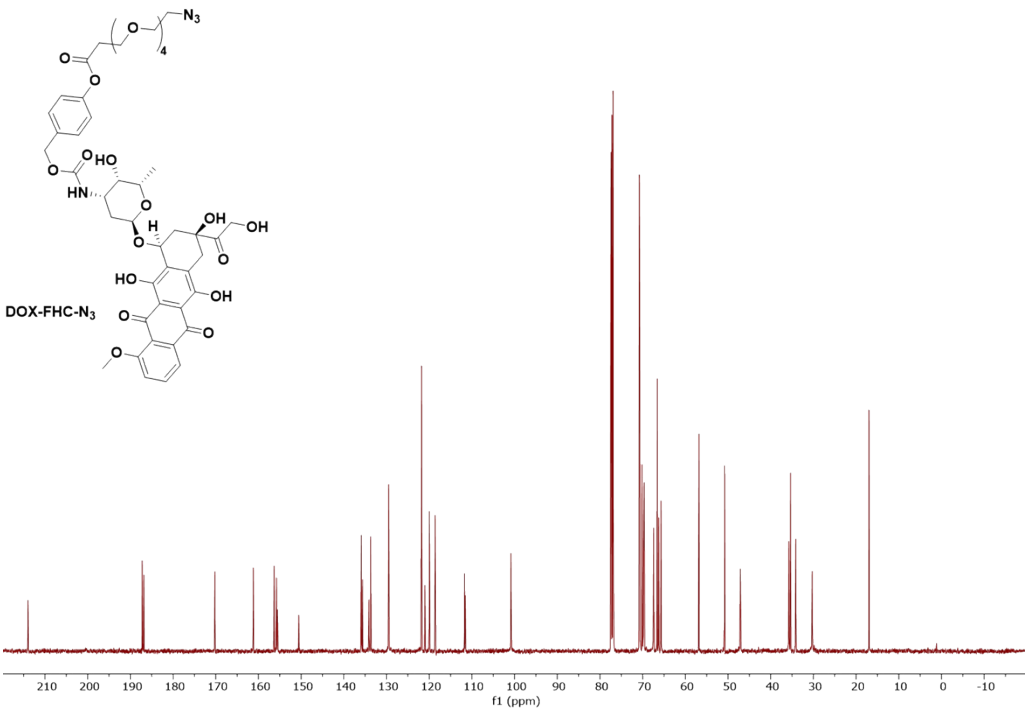

Figure S39. ^{13}C NMR Spectrum of **DOX-FHC-N_3** in $CDCl_3$

Spectra Data for DOX-SHC-N_3

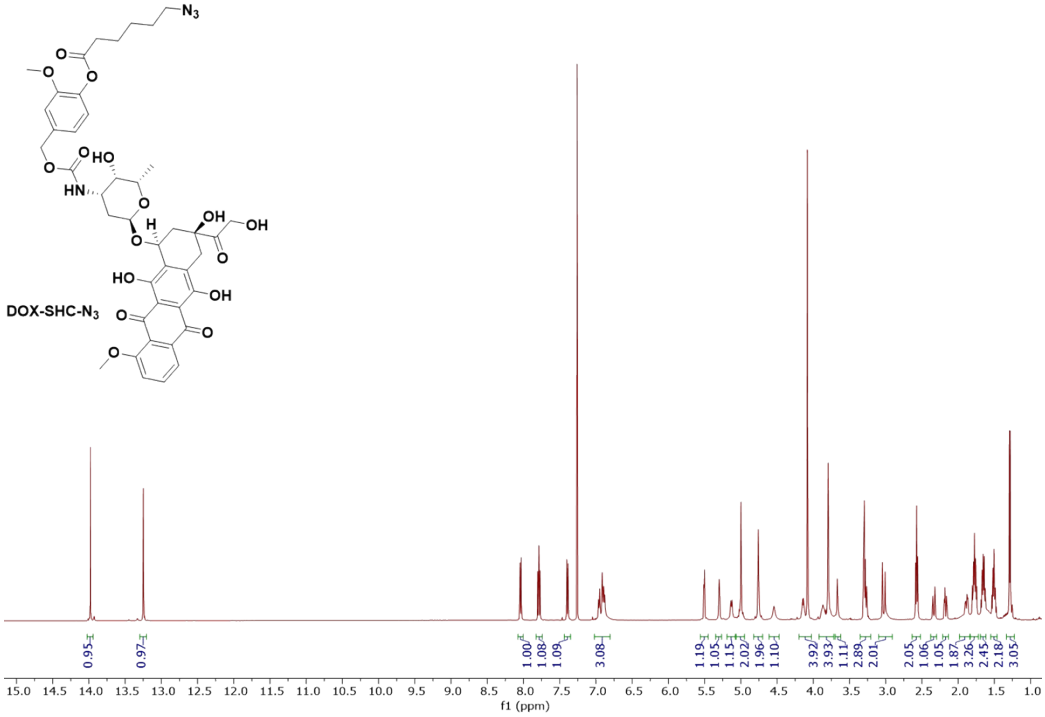

Figure S40. ^{1}H NMR Spectrum of **DOX-SHC-N_3** in $CDCl_3$

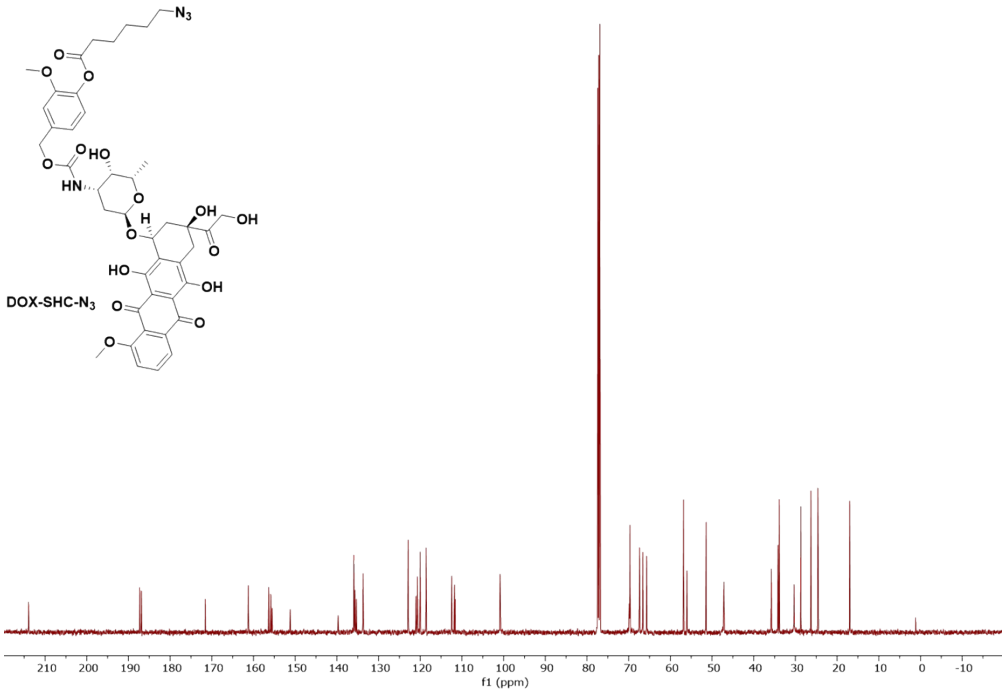

Figure S41. ^{13}C NMR Spectrum of **DOX-SHC-N_3** in $CDCl_3$

Section E. Supplementary References

1 Love, J. A.; Morgan, J. P.; Trnka, T. M.; Grubbs, R. H. A Practical and Highly Active Ruthenium-Based Catalyst that Effects the Cross Metathesis of Acrylonitrile. *Angew. Chem. Int. Ed.* **2002**, *41*, 4035–4037.

2 Sowers, M. A.; McCombs, J. R.; Wang, Y.; Paletta, J. T.; Morton, S. W.; Dreaden, E. C.; Boska, M. D.; Ottaviani, M. F.; Hammond, P. T.; Rajca, A.; Johnson, J. A. Redox-Responsive Branched-Bottlebrush Polymers for *In Vivo* MRI and Fluorescence Imaging. *Nat. Commun*. **2014**, *5*, 5460.

3 Liao, L.; Liu, J.; Dreaden, E. C.; Morton, S. W.; Shopsowitz, K. E.; Hammond, P. T.; Johnson, J. A. A Convergent Synthetic Platform for Single-Nanoparticle Combination Cancer Therapy: Ratiometric Loading and Controlled Release of Cisplatin, Doxorubicin, and Camptothecin. *J. Am. Chem. Soc*. **2014**, *136*, 5896–5899.

4 Gao, A. X.; Liao, L.; Johnson, J. A. Synthesis of Acid-Labile PEG and PEG-Doxorubicin-Conjugate Nanoparticles *via* Brush-First ROMP. *ACS Macro Lett*. **2014**, *3,* 854–857.

5 Nguyen, H. V.-T.; Gallagher, N. M.; Vohidov, F.; Jiang, Y.; Kawamoto, K.; Zhang, H.; Park, J. V.; Huang, Z.; Ottaviani, M. F.; Rajca, A.; Johnson, J. A. Scalable Synthesis of Multivalent Macromonomers for ROMP. *ACS Macro Lett*. **2018**, *7*, 472-476.

6 Rajca, A.; Wang, Y.; Boska, M.; Paletta, J. T.; Olankitwanit, A.; Swanson, M. A.; Mitchell, D. G.; Eaton, S. S.; Eaton, G. R.; Rajca, S. Organic Radical Contrast Agents for Magnetic Resonance Imaging. *J. Am. Chem. Soc*. **2012**, *134*, 15724-15727.

7 Nguyen, H. V.-T.; Chen, Q.; Paletta, J. T.; Harvey, P.; Jiang, Y.; Zhang, H.; Boska, M. D.; Ottaviani, M. F.; Jasanoff, A.; Rajca, A.; Johnson, J. A. Nitroxide-Based Macromolecular Contrast Agents with Unprecedented Transverse Relaxivity and Stability for Magnetic Resonance Imaging of Tumors. *ACS Cent. Sci.* **2017**, *3*, 800-811.